KU ScholarWorks

Identification of negative regulators of p53 pathway by a forward genetic screen in ovarian cancer

Item Type	Thesis
Authors	Minn, Kay T.
Publisher	University of Kansas
Rights	Copyright held by the author.
Download date	2024-08-20 21:43:53
Link to Item	https://hdl.handle.net/1808/30115

Identification of negative regulators of p53 pathway by a forward genetic screen in ovarian cancer

By

© 2018

Kay T. Minn
B.Sc., University of Kansas 2003

Submitted to the graduate degree program in Pathology & Laboratory Medicine and the Graduate Faculty of the University of Kansas in partial fulfillment of the requirements for the degree of Master of Science.

Chair: Jeremy Chien, PhD

Co-Chair: Andrew K. Godwin, PhD

Fariba Behbod, PharmD, PhD

Joan Lewis-Wambi, PhD

Date Defended: 26 November 2018

The thesis committee for Kay T. Minn certifies that this is the
approved version of the following thesis:

Identification of p53 negative regulators in p53-network by forward genetic screening in ovarian cancer

Co-Chair: Jeremy Chien, PhD

Co-Chair: Andrew K. Godwin, PhD

Date Approved: 30 November 2018

Abstract

Ovarian cancer is the deadliest of all female gynecological cancers and the fifth leading cause of cancer-related death in women. Lack of early detection and treatment failure are the major contributors to ovarian cancer death in women. Understanding ovarian cancer at the molecular level will help provide better treatment options, such as targeted therapies. Nearly sixty percent of women are diagnosed at late stage ovarian cancer. *TP53* is the most commonly mutated gene in ovarian cancer as well as in all other cancers. However, there are subsets of ovarian cancer patients with wild-type *TP53,* and we would like to understand the molecular and cellular mechanisms that disable the transcriptional functions of p53 in those patients. Wild-type p53 is the transcription factor that activates sets of genes to respond to various types of cellular and molecular stress and to maintain genomic stability in normal cells. The major function of wild-type p53 is the transcriptional activation of genes that are involved in cell cycle arrest to repair DNA damage and cell death if the damage is beyond repair in cells. However, the p53 transcriptional functions of cell cycle arrest and cell death are not observed in those ovarian cancer patients with wild-type *TP53* and the genes inhibiting transcriptional activities of p53 are not well studied. Additionally, our understanding of negative regulators of p53 in cell activity is not complete, and identifying those regulators may provide new insights into how the p53 pathway can be deregulated in tumors without mutations in *TP53*. For that purpose, we performed forward genetic screening using a patient-derived pool cDNA library constructed with pRetro-LIB vector in wild-type *TP53* ovarian cancer cells to identify the potential negative regulators of p53.

First, we tested our method of screening in wild-type *TP53* ovarian cancer cells to prove the concept of our experimental approach. We found that using modified 293T cells (Phoenix AMPHO) with spin-fection method overcame the low transfection efficiency of retroviral particles in wild-type *TP53* ovarian cancer cells (A2780). In normal cells, p53 is present at relatively low levels because of the negative feedback loop between Mdm2 and p53. To induce the p53 level in ovarian cancer cells with wild-type *TP53*, we used the small molecule inhibitor, Nutlin-3a. Nutlin-3a blocks the interaction between Mdm2 and p53, thereby allowing the stabilization of p53 in ovarian cancer cells. Stabilized p53 transactivates genes that initiate cell cycle arrest or cell death. Accordingly, Nutlin-3a suppresses the growth of cancer cells with wild-type *TP53*. We used this system to screen for exogenous genes from the patient-derived cDNA library that block Nutlin-3a-mediated growth suppression in A2780 cancer cells.

The screen identified three candidate genes (*NIFK*, *GXYLT* 1, and *SACS*) that prevent the Nutlin-3a-induced growth suppression in A2780 cancer cells, and NIFK (also known as Nucleolar Protein Interacting with the FHA Domain of MKI67 or *MKI67IP*) was identified in four independent screening experiments. *NIFK* encodes a protein that interacts with the forkhead-associated domain of the Ki-67 antigen and has been implicated in ribosome biogenesis, *e.g.,* pre-ribosomal RNA processing and ribosome assembly. NIFK also associates with pre-mRNAs. However, the potential association between NIFK and p53 in ovarian cancer is unknown. We evaluated the level of NIFK, p53, and Mdm2 in NIFK-overexpressing ovarian cancer cells. We found that the dose-dependent effect of NIFK expression in preventing the Nutlin-3a-induced growth suppression in A2780 cells. Our results suggest that NIFK overcomes

the growth arrest by functional p53 induced by Nutlin-3a, and NIFK negatively regulates p53 pathway in ovarian cancer cells.

In summary, our studies showed that NIFK overexpression cells play a role in cell survival, proliferation and the negative regulation of p53 in ovarian cancer cells, and this should be further explored to understand the molecular function of NIFK.

Acknowledgments

I would like to thank all the members of my thesis committee, Dr. Andrew K. Godwin, Dr. Jeremy Chien, Dr. Joan Lewis-Wambi and Dr. Fariba Behbod for their time, excellent suggestions and overall support to this thesis.

I am grateful to my co-mentor Dr. Jeremy Chien for his intellectual input, encouragement, and suggestions. His enthusiasm for science and his passion for research encouraged me to continue with the project during those difficult times. His mentorship has allowed me to be a very independent researcher and has helped me to understand why I need to perform experiments to test my scientific hypothesis. He has guided me through the up and down moments of those experiments to reach the goal of this project.

I would like to thank Zoë Baldwin for all her help from the first day of my graduate studies and her willingness to help me with all the registration problems during enrollment time. She also makes sure that I am always on track with graduation requirements and tirelessly answers all my questions. I sincerely thank her for all her help throughout my graduate school years.

I also want to thank all out a great group of past and present lab members and it is my pleasure to work with a team of people who really care and help one another to support and encourage me while going through the journey. We had so much fun in the lab as well as in all social gatherings and Happy Hours. I want to thank Megan Cooley for showing me that I can have a good friendship with people with whom I work. I admire her willingness to take on the tasks in the lab that I do not wish to deal with, namely the pH meter and pH adjustment in buffers. I thank Pingping for being a good friend with whom to discuss either techniques or

approaches of experiments. We had good and bad times together but still had fun and good friendship that I can care for. I thank Prabhakar for his criticisms of my experiment results, the coffee run, and his dry sense of humor as the occasion arose. Being in the lab with such the wonderful people and an excellent work environment, I cannot ask for more as the graduate student. I thank them all for sharing my thoughts not only in research projects but also in personal life. I am fortunate enough to share my graduate study years with them and thank them for their kindness, trust, and friendship that will last beyond graduate study years.

My special thanks go to my parents, siblings and my aunts who are always there for me unconditionally. Without their support, I would not have gotten this far. They have shown me the wise path to walk in my life and guided me to become a better person. They supported me throughout those years and define me as I am today.

My wonderful and kind husband Jeremy, who encouraged and provided me with the chance to go back to study and made this work possible, thank you. You are such a good scientist who would like to explore everything based on the experimental results and have many great ideas about the projects. Your excitement about projects as well as findings regardless of negative or positive results and your willingness to teach students will always remind me why I have to learn constantly in the field to update my knowledge. Your dedication to a better understanding of the mechanisms of cancer in patients helps me understand why I am doing research in ovarian cancer. You inspire me and remind me why I do what I do daily. To my special daughter, Aeakri, you are the unique person who helps me with everything that I need to go through the journey.

Dedicated

To my mother who supported me for everything especially in education

To my father who teaches me to see the world in very different view

To my siblings who argue with me and still love and care for me

To my two aunts who care, love and support me with everything they can

To my grandparents who migrated to another country for the better future

&

To my beloved husband and daughter who know me and fill me with happiness and joy, as well as support with all their love

Table of Contents

List of Abbreviations

A2780	=	Cell line, human ovarian carcinoma
ATM	=	Ataxia Telangiectasia (ATM) gene
ARID1A	=	AT-rich interactive domain-containing protein 1A
BER	=	Base-excision repair
BRAF	=	Gene encodes B-Raf protein
BRCA1	=	Breast Cancer Type 1 susceptibility protein
BRCA2	=	Breast Cancer Type 2 susceptibility protein
CA125	=	Cancer antigen 125
CT	=	Compound tomography
CTNNB1	=	Catenin (Cadherin-Associated Protein), Beta 1
copies/mL	=	Viral RNA copy number per milliliter
DNA	=	Deoxyribonucleic acid
DNA-PK	=	DNA-dependent protein kinase
EOC	=	Epithelial ovarian cancer
ERBB2	=	Gene encodes receptor tyrosine protein kinase erbB-2
FBS	=	Fetal bovine serum
FIGO	=	Federation of Gynecology and Obstetrics
GADD45	=	The Growth Arrest and DNA Damage
gDNA	=	Genomic DNA
GXYLT1	=	Glucoside Xylosyltransferase 1
HGSC	=	High-grade serous carcinoma

KRAS	=	Proto-oncogene identified in Kirsten rat sarcoma virus
M199/M105	=	Culture media for A2780 cell line
MKI67IP	=	Ki-67 interacting protein
MOI	=	Multiplicity of infection
MRI	=	Magnetic resonance imaging
NES	=	Nuclear export signal sequence
NGS	=	Next generation sequencing
NLS	=	Nuclear localization signal sequence
NIFK	=	Nucleolar protein interacting with the FHA domain of Ki-67
Opti-MEM	=	Opti-MEM, a reduced serum medium
PBS	=	Phosphate buffered solutions
Pen/strep	=	Penicillin-streptomycin solution
pfu/mL	=	plaque forming unit (pfu) of virus used for infection per milliliter
PIK3CA	=	Phosphoinositide 3-kinase catalytic subunit alpha isoform gene
PTEN	=	Gene encodes phosphatase and tensin homolog (PTEN)
qRT-PCR	=	Reverse transcriptase real-time quantitative PCR
RING	=	Really interesting new gene
RNA	=	Ribonucleic acid
siRNA	=	Small interference RNA
SACS	=	Gene that encodes for Sacsin protein
STIC	=	Serous tubal intraepithelial carcinoma
TCGA	=	The Cancer Genome Atlas

TIC   =   Tubal intraepithelial carinoma

TP53   =   Gene that encodes for tumor suppressor protein p53

pRetro-LIB   =   The retroviral vector used in generating the patient-derived cDNA

            library

List of Figures

List of Tables

Chapter 1: Background and Introduction

Introduction

1.1 Ovarian cancer

Ovarian cancer ranks fifth in cancer deaths and is accountable for more than other female reproductive-related cancer deaths in the United States alone (American Cancer Society). The lifetime risk for a woman of having ovarian cancer is 1 in 78 or 1.3% in women, and the median age of a person with ovarian cancer at the time of diagnosis is 63 years (Siegel et al., 2018). There are no obvious risk factors that are related to ovarian cancer and the only known strongest risk factor is a family history of breast and ovarian cancer (Siegel et al., 2018). According to the American Cancer Society, there will be approximately 22,240 new cases of ovarian cancer diagnosed in 2018 and 14,070 ovarian cancer-related death in the U.S. alone. Currently, ovarian cancer is accountable for 2.5% of all cancer cases, but 5% of all cancer-related deaths in females (Siegel, Miller, and Jemal 2018).

Ovarian cancer is the most lethal gynecologic cancer among women's cancers due to the lack of early detection, limited understanding of disease origin and no effective treatment for the disease. Early detection is still a challenge in ovarian cancer because the disease is normally asymptomatic before the tumor is spread to other distant organs such as bowel and omentum (George, Garcia, and Slomovitz 2016). The quest for the discovery of precursor lesions in ovarian cancer has not been successful regardless of numerous studies, which suggests that ovarian cancer develops *de novo* (Kurman and Shih Ie 2010). The origin of an ovarian tumor is still under debate. It was believed that ovarian cancer originates from the ovarian epithelium and different progenitor cell types resulting from metaplastic changes (Kurman and Shih Ie 2010). This understanding has been challenged in recent years, suggesting that the ovarian cancer is

derived from Mullerian-type tissue and not from the ovarian surface epithelium (Kurman and Shih Ie 2010).

It is not surprising that ovarian cancer is a compound disease due to its structures. The ovary is a complex organ and composed of various cell types for specific functions to support structure, hormone production, and reproduction. Ovarian cancer can be generally categorized into three main different types: sex cord-stromal tumors, germ cell tumors, and epithelial ovarian cancer (George, Garcia, and Slomovitz 2016). Epithelial ovarian cancer accounts for more than 90% of all ovarian cancer cases, while germ cell and sex cord-stromal ovarian cancer account for 3% and 2% of cases respectively (Figure 1.1.1) (Siegel, Miller, and Jemal 2018). Germ cell ovarian cancers originate from the germ cells of the ovary. The origin of sex cord-stromal ovarian cancers is from the other supportive cells in the ovarian follicles. The origin of epithelial ovarian cancer is unresolved and an issue of a longstanding debate.

Epithelial ovarian cancer (EOC) can be delineated into different histologic subtypes: mucinous (6%), endometrioid (10%), clear cell (6%), and serous carcinoma (52%) (Erickson, Conner, and Landen 2013). The serous tumors are thought to originate from the epithelial cells of the fallopian tube and later migrate to the ovaries (Siegel, Miller, and Jemal 2018). The endometrioid and clear cell tumors originate in the endometrium. Mucinous tumors are from the fallopian tube-peritoneal junction or the ovaries (Siegel, Miller, and Jemal 2018). The serous carcinoma can be further divided into (1) high-grade or (2) low-grade serous carcinoma.

Based on morphologic, immunohistochemical, and molecular genetic studies, epithelial ovarian cancer can be categorized into type I or type II ovarian cancer (Kurman and Shih Ie 2011). Type I tumors present at a low stage, and the disease progresses in a stepwise manner

(Jones et al. 2012). Type I tumors that are confined to the ovary have a good prognosis, although advanced stage type I tumors have a poor outcome (Kurman and Shih Ie 2016). Type I ovarian tumors are divided into three groups: endometriosis-related tumors, low-grade serous carcinomas, mucinous carcinomas and malignant Brenner tumors (Kurman and Shih Ie 2016). Type I endometriosis-related tumors include endometrioid, clear cell, and seromucinous carcinomas (Kurman and Shih Ie 2016). Genetic mutations such as *KRAS*, *BRAF*, *PTEN*, *PIK3CA*, *ERBB2*, *ARID1A,* and *CTNNB1* are common in type I ovarian cancers, but *TP53* mutations are very rare (Kurman and Shih Ie 2011). Type II ovarian tumors are normally high-grade serous carcinoma, high-grade endometrioid carcinoma, malignant mixed mesodermal tumors, and undifferentiated carcinomas. Type II ovarian cancers are highly aggressive and normally present in advanced stages. A typical "tubal intraepithelial carcinoma" (TIC) and "serous tubal intraepithelial carcinoma" (STIC) are observed in ovarian high-grade serous carcinomas in both women with inherited *BRCA1* or *BRCA2* mutations and women without a known predisposing genetic mutation for ovarian cancer (Kurman and Shih Ie 2016). Type II ovarian cancers harbor *TP53* mutations in almost all tumors according to The Cancer Genome Atlas (TCGA) project of ovarian cancer (Kurman and Shih Ie 2016). In addition, DNA copy number gains or losses in *CCNE1*, *NOTCH3*, *AKT2*, *RSF1*, and *PIK3CA* are other molecular features of type II high grade serous ovarian cancer (Kurman and Shih Ie 2011). The term "p53 signatures" is used to describe the high-intensity immunostaining for p53 in STICs and *TP53* mutations are associated with the p53 signatures in some STICs (Kurman and Shih Ie 2011).

The main reason to analyze epithelial ovarian cancers into type I and type II groups is the relation of the different histologic subtypes to precursor lesions (Kurman and Shih Ie 2016). In

type I epithelial ovarian cancers developed from well-established benign precursor lesions of borderline or atypical proliferative tumors (Kurman and Shih Ie 2016). There is no precursor lesion in type II epithelial ovarian cancers and considered as de novo development (Kurman and Shih Ie 2016). The studies have shown that type II carcinomas develop from an intraepithelial carcinoma in the fallopian tube, located in the fimbria and designated as STIC in the past few years (Kurman and Shih Ie 2016).
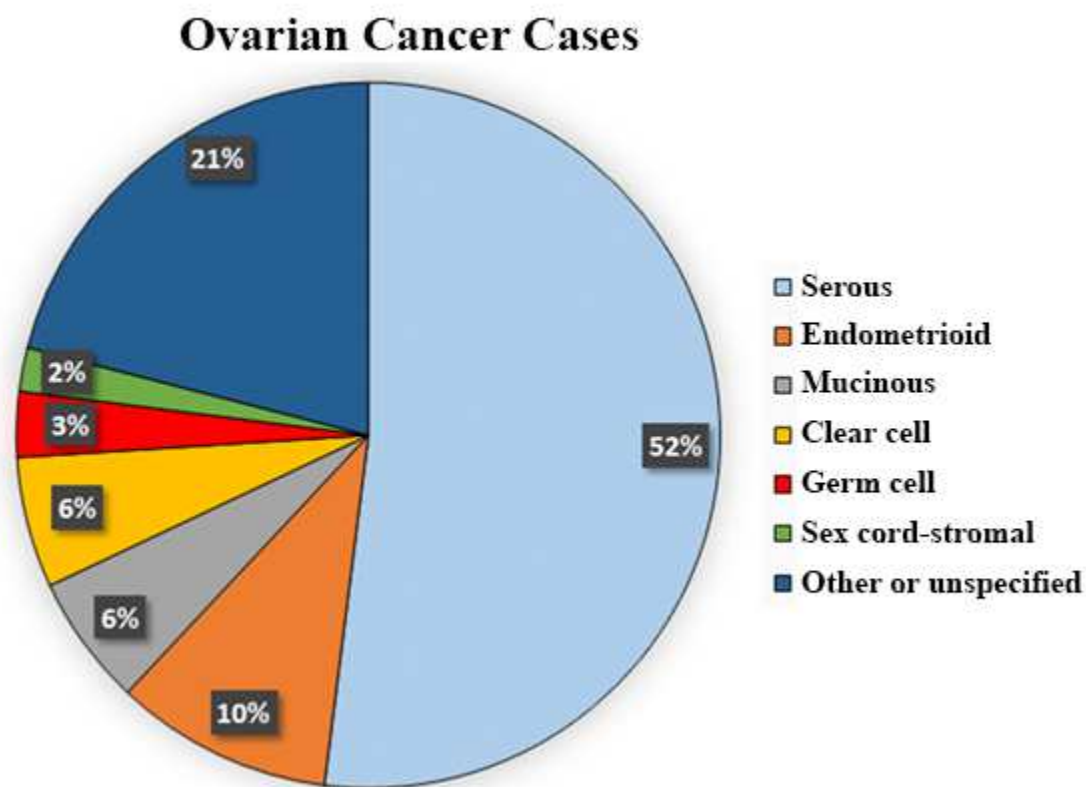
Figure 1.1.1. Percent distribution of different ovarian cancer cases by subtypes. *The pie chart represents the distribution of ovarian cancer cases by subtypes in the United States. Other or unspecified subtype includes very low occurring ovarian tumors as well as tumors that are hard to categorize based on the histological phenotype. Source: North American Association of Central Cancer Registries (NAACCR), 2017.*

1.1.1: Ovarian cancer stages

As with other cancers, the outcome of ovarian cancer in patients is dependent upon the stage of disease at the time of diagnosis. International Federation of Gynecology and Obstetrics (FIGO) staging system is a standardized method for the staging of ovarian tumors once the patient is diagnosed with the disease (Prat 2015). The additional discovery of high-grade serous tubal intraepithelial carcinoma (STIC) along with different tumor histopathological tissues is expected to modify the stages of ovarian cancer (Prat 2015). According to the new updated staging system of ovarian cancer, the stages of ovarian cancer are as follows:

Stage I – Tumor is confined only to either ovaries or fallopian tubes.

Stage II – Tumor involves either one or both ovaries or fallopian tubes with a pelvic extension or primary peritoneal cancer.

Stage III – Tumor involves either one or both ovaries or fallopian tubes, or primary peritoneal cancer, with cytologically or histologically confirmed spread to the peritoneum outside the pelvis and/or metastasis to the retroperitoneal lymph nodes.

Stage IV – Tumor is metastasized to distant organs excluding peritoneal metastases.

1.1.2: Ovarian cancer symptoms

Common symptoms of ovarian cancer are often mistaken with digestive disease and include abdominal bloating, indigestion, nausea, increased abdominal girth, tiredness and loss of appetite. Those whispering symptoms have made the diagnosis of ovarian cancer challenging and frequently misread as indigestion by patients. If the patient is suspected with the disease,

physical examination along with blood tests and imaging computed tomography (CT) scan or magnetic resonance imaging (MRI) are part of the tools for diagnosing ovarian cancer (Siegel, Miller, and Jemal 2018). The two most commonly used screening methods in ovarian cancer are a transvaginal ultrasound and the cancer antigen 125 (CA125) blood test. The CA125 levels often drop with decreased ovarian tumor mass, and it surrogate biomarker to monitor disease progression after treatment rather than the diagnostic test for ovarian cancer. Although a transvaginal ultrasound and the CA125 blood tests are extensively used in clinics to detect ovarian cancers in women, the methods are not reliable to detect early disease in patients. Randomized clinical trials assessing the efficacy of cancer antigen CA125 and transvaginal ultrasound on ovarian cancer mortality demonstrated that there was no difference between control and test groups (Buys et al. 2011) (Skates et al. 2017). The control group did not receive annual screening such as CA125 blood test and transvaginal ultrasound, while the test group received the annual screening for ovarian cancer (Buys et al. 2011).

1.1.3: Ovarian Cancer treatment

The standard treatment procedures for patients with advanced ovarian cancer are as follows:

1. Optimal debulking surgery: The surgery procedure to remove all tumors larger than 1 cm (Altman et al., 2012). This includes removing the uterus (hysterectomy) or both ovaries and fallopian tubes (bilateral salpingo-oophorectomy) if the pathology test is positive for the presence of a tumor.

2. Chemotherapy: Chemotherapy given for ovarian cancer is generally a combination of platinum- or taxane-based drugs administered intravenously based on the recommended dose by the oncologist. Currently, the standard chemotherapy regimen includes a platinum compound such as cisplatin or carboplatin and a taxane agent such as paclitaxel or docetaxel (Akin et al., 2014; Sharma et al., 2009).

3. Targeted therapy: Targeted therapy is a promising strategy to treat ovarian cancer patients because there is little or almost no damage to normal cells. The targeted therapies are either drugs or other agents that attack cancer cells only. There are limited FDA-approved target therapies and clinical trials of specific targeted therapies in ovarian cancer in recent years. The examples of these targeted therapies are the angiogenesis inhibitor bevacizumab (McClung and Wenham, 2016; Pujade-Lauraine et al., 2014) and PARP inhibitors olaparib, rucaparib, and niraparib (Bamford and Webster, 2017) (Mirza et al. 2016) for patients with hereditary BRCA mutations or somatic BRCA mutations. Tazoparaib and Veliparib are other PARP inhibitors and testing in early clinical trial (Mittica et al. 2018). Clinical trials are on the way to investigate the effectiveness of combination treatment with these agents together with standard chemotherapy and immunotherapies or maintenance therapy or monotherapy in a wide range of settings in ovarian cancer (Mittica et al. 2018) (Mirza et al. 2016).

The National Cancer Institute (NCI) defined ovarian cancer as cancer that is formed in the tissues of the ovary. The multiple studies of ovarian cancer have demonstrated that ovarian cancer is a heterogeneous disease with different origins (Levanon, Crum, and Drapkin 2008). Molecular genetic studies have revealed that the origin of ovarian cancer is not primarily in the

ovaries, and more than one test is required to detect all different types of ovarian carcinomas (Kurman and Shih Ie 2011). The current treatment for ovarian cancer mainly depends on the stage of cancer, tumor characteristics, and subtype (Siegel, Miller, and Jemal 2018). Based on the recent literature, treatment for ovarian cancer should be modified in every patient according to the molecular mutations, pathway inactivation of the patient's tumor type and sub-type of the disease (Kurman and Shih Ie 2011).

1.2 The guardian of the genome: p53 protein

The different studies of *TP53* have led to identifying the encoded protein as a tumor antigen, an oncogene or a tumor suppressor (Levine, Momand, and Finlay 1991). The *TP53* gene was first discovered in the transformed cells interacting with antiserum from animals with tumors induced by simian virus 40 (SV40) (Levine, Momand, and Finlay 1991). The *TP53* was found in the transformed cells together with large T-antigen, which was required for the transformed phenotype, and was identified as an oncogene. The initial *TP53* cDNA clones used in these studies were the mutant forms of the gene, and a later cloning and characterization of the wild-type *TP53* firmly established its role in suppressing the growth of transformed cells (Levine, Momand, and Finlay 1991). As a result, wild-type *TP53* is now characterized as a tumor suppressor due to its ability to suppress oncogenic activities (Oren 1999). The *TP53* tumor suppressor gene encodes the p53 protein, and p53 plays a critical role in maintaining the integrity of the genome by controlling the cell cycle and cell death to prevent tumorigenesis in normal cells (Vogelstein, Lane, and Levine 2000). The p53 protein responds to the various stress signals

in cells, including DNA damage that can lead to replication stress, hypoxia, nutrient deprivation, ribosomal stress, and oncogenic activations.

p53 Protein Structure
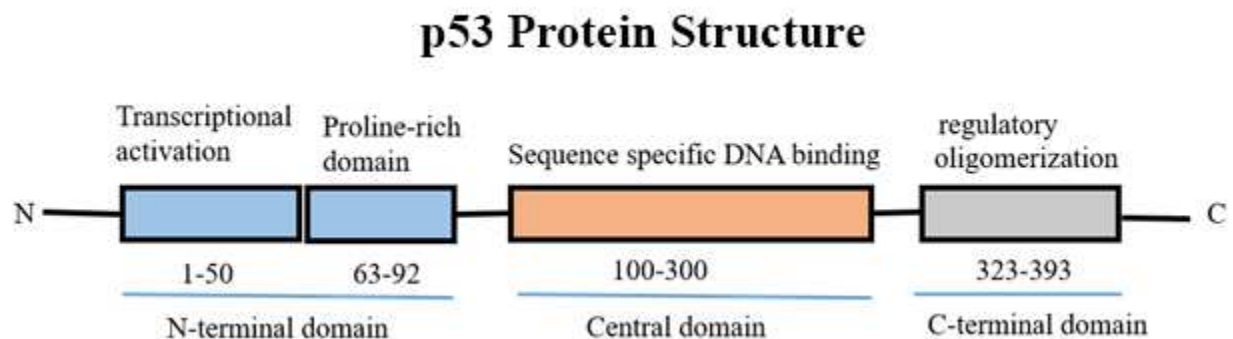
Figure 1.2.1. Schematic diagram of p53 protein structure. *The p53 protein is 53kDa and has four functional structure domains. The N-terminal domain contains a transcriptional activation domain and Proline-rich domain. The central domain is where sequence-specific binding with the target genes and the other proteins can bind p53 at the C-terminal domain for regulation of genes in its network.*

The human *TP53* gene is approximately 20 kb long and is located on the short arm of chromosome 17. The *TP53* gene has 11 exons and the gene has maintained highly conserved sequences throughout its evolution (Soussi et al. 1987). The p53 protein is export from the cytoplasm to the nucleus where it forms a dimer of dimer and becomes an active transcription factor. The human p53 protein has 393 amino acids and contains four functional domains (Levine 1997). The four functional domains are (1) transcriptional activation domain, (2) proline-rich domain, (3) sequence-specific DNA binding domain in the center and (4) oligomerization and regulatory domains at the C-terminus.

The transcriptional activation domain is at the N-terminus, and it is required for interacting with basal transcriptional machinery to regulate genes expression in normal cells (Levine 1997). For example, the p53 amino acids F19, L22 and W23 are required for binding of

TATA-associated factors (Thut et al. 1995), and the p53 amino acid residues 22 and 23 are required for the binding of Mdm2 protein (Levine 1997). The N-terminal domain of p53 protein has binding sites for both positive and negative regulation of p53-dependent transcriptional activities (Levine 1997). The regulations of p53 are mainly through post-translational modifications and some of those modifications are at the N-terminal of the protein. Phosphorylation of p53 at the S46 position is required to induce the pro-apoptotic gene *AIP-1* after UV treatment *in vivo* (Oda et al. 2000). AMPK (Okoshi et al. 2008) and DYRK-2 (Taira et al. 2007) can bind to p53 at the same position of S46 amino acid residue and activate genes that are involved in cell death. In addition, the nuclear localization signal of the p53 protein is located in the N-terminal domain.

The DNA binding domain of p53 protein interacts with DNA in a sequence-specific manner, and the mutations in this domain can disrupt the binding of the p53 protein to its target genes (Levine 1997) (May and May 1999). The majority of cancer-associated mutations in *TP53* are point mutations that lead to a single amino acid substitution in the DNA binding domain (Vousden and Lu 2002) and these types of mutations are called missense mutations. Furthermore, the mutations in DNA binding domain can divide into two classes: (1) mutations that directly interfere with the sequence-specific DNA binding (so called "contact mutants") and (2) mutations that lead to conformational changes of p53 protein (so called "conformational mutants") (Levine 1997). Unlike mutations in other genes, the DNA contact mutations of *TP53* can sometimes retain the mutant/wild-type p53 complexes and can interfere with wild-type p53 functions. Structural mutations change the p53 protein conformation, and the mutated p53 protein can then bind to other proteins which are not observed with the wild-type p53. The DNA

binding domain of p53 recognizes and binds to a consensus target sequence (el-Deiry et al. 1992). The central domain of p53 also interacts with other proteins such as *53BP1* and *53BP2* (Ruppert and Stillman 1993) and functions as the protein bind domain for the p53 protein.

The oligomerization domain (amino acid residues 324-355) of the p53 protein is required for the tetramerization in normal cells. The formation of a dimer of a dimer protein structure is necessary to regulate the ability of p53 to assist the binding of specific DNA sequences at its core domain (Levine 1997). The C-terminal domain of p53 is subjected to the post-translational modifications and interacts with other regulatory proteins to maintain genomic stability in normal cells (Levine 1997).

The p53 protein is not required for the normal functions of cells within the body as evidenced by the p53 knockout mice having normal development and maturation processes (Oren 1999). The broad range of stress that leads to genomic instability is the key to carcinogenic mechanisms and those events will trigger the activation of p53 in cells (Oren 1999). The activation of p53 happens in three steps: (1) the stabilization and accumulation of p53 in the cell; (2) sequence-specific DNA binding to target genes; and (3) target gene activation in response to the stress in the normal cells (Kruse and Gu 2009). From the functional aspect, p53 protein is the transcription factor that can regulate the expression of genes involved in cell cycle and growth arrest or cell death. The N-terminal transcription activation domain and a DNA sequence-specific DNA binding domain are required for the p53 transcriptional activities (Chen, Lin, and Levine 1995). The first step of p53-mediated activation in target genes is binding of the protein to the specific sequence in DNA, and it is not surprising that the majority of p53

missense mutations are located in the DNA binding domain of the protein (Beckerman and Prives 2010).

1.3 The negative regulator of p53: Mdm2

The *MDM2* (murine double minute 2) gene is approximately 42 kb long and has eleven coding exons. There are two different promoters for the *MDM2* gene leading to the different transcripts (Barak et al. 1994). The largest human MDM2 protein consists of 491 amino acids and contains domains conserved among species from human to zebrafish (Marechal et al. 1997). The conserved region at the N-terminal domain of the MDM2 interacts with p53 and inhibits the p53 transcriptional activation functions (Chen, Marechal, and Levine 1993). Another conserved nuclear localization sequence (NLS) and nuclear export signal sequence (NES) facilitate the proper nuclear-cytoplasmic trafficking of the MDM2 protein (Roth et al. 1998). Those signals are required and essential for the Mdm2 to regulate p53 protein levels in cells (Roth et al. 1998). The conserved region at the C-terminal domain of MDM2 has the caspase 3 cleavage site (Chen et al. 1997) and three putative DNA protein kinase (DNA-PK) phosphorylation sites (Marechal et al. 1997). The two conserved zinc fingers region in the C-terminal RING (Really Interesting New Gene) domain are required for the binding of zinc molecules and the proper folding of the RING domain. The conserved regions in the RING domain bind to a specific RNA sequence and probably play a role in the regulation of p53 (Honda, Tanaka, and Yasuda 1997). The amino acid residues G58, V75, D68 and C77 on the Mdm2 protein are critical for binding to p53 protein, and the mutation in those amino residues could result in the disruption of interaction between MDM2 and p53 (Kussie et al. 1996).

MDM2 Protein Structure
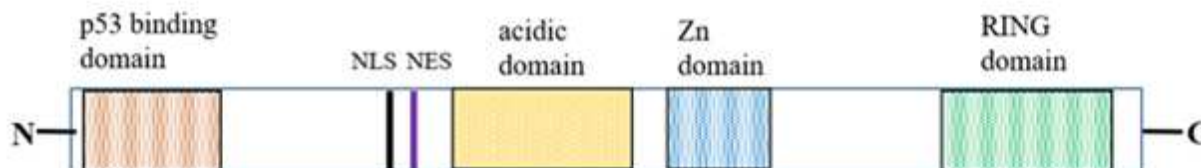
Figure 1.3.1. Schematic diagram of MDM2 protein structure. MDM2 interacts with p53 at N-terminal and p53 DNA binding domain located between the acidic domain and Zn domain. There are Nuclear Localization Signal (NLS) and Nuclear Export Signal (NES) to transport MDM2 protein from cytoplasm to nucleus and vice visa. The Zn and RING domains of MDM2 interact with other proteins.

MDM2 inhibits p53's transcriptional functions by several different mechanisms. First, MDM2 blocks the transcriptional activities of p53 by competing with TFIID transcription factor complex and leads to transcriptional suppression of the downstream target genes in the p53 pathway. The binding of MDM2 to p53 leads to a decrease in the activation of p53-responsive reporter genes in both mammalian cells and in yeast (Chen, Lin, and Levine 1995). The transcriptional activities of p53 in the absence of MDM2 can be explained in the MDM2 knockout mice model. MDM2 homozygous knockout mice are embryonically lethal, and the lethality phenotype can be rescued by the additional homozygous deletion of p53 gene. The transcriptional activities of p53 in the absence of regulation of MDM2 results in embryonic lethality in the knock out mice model (Jones et al. 1995) (Montes de Oca Luna, Wagner, and Lozano 1995). Second, MDM2 can regulate the endogenous p53 protein level in both the wild-type and heterozygous mutant (Haupt et al. 1997) (Kubbutat, Jones, and Vousden 1997). The decrease in endogenous p53 levels is not dependent upon the transcription of p53 genes or mRNA, but the ability of MDM2 to transport p53 protein from the nucleus to the cytoplasm for

ubiquitinated degradation (Roth et al. 1998). MDM2 is an E3 ubiquitin ligase that binds to the p53 protein to target for proteasomal degradation in the cytoplasm (Honda, Tanaka, and Yasuda 1997). By targeting p53 for degradation, MDM2 effectively inhibits all activities of p53 in cells. For example, MDM2 inhibits p53-mediated transcriptional activation but does not prevent transcription-independent function of p53, such as an enhancement of DNA repair or the induction of apoptosis. To inhibit all p53 transcription-dependent and -independent activities of p53, including base-excision repair (BER), DNA double-strand exonuclease activity, and p53-mediated cell death, the proteasomal degradation of p53 by MDM2 is the most effective method to inhibit all p53 activities (Honda, Tanaka, and Yasuda 1997) (Roth et al. 1998).

1.4 The p53-MDM2 autoregulatory feedback loop

In normal and non-malignant cells, the level of p53 is very low due to the protein's short half-life regulated by MDM2. The p53 protein transactivates MDM2 transcription and MDM2 in turn ubiquitinates p53 and facilitates the degradation of p53. This autoregulatory negative feedback loop controls the basal level of both p53 and MDM2 proteins. In normal cells, maintenance of autoregulatory feedback is necessary to overcome the inhibition of p53 by MDM2 under certain circumstances. One of the mechanisms to regulate the autoregulatory feedback loop is to lower Mdm2 protein level. Another mechanism is to block the interaction of p53 and MDM2 by blocking with the small molecule inhibitor to activate p53 transcriptional activities.

P53-MDM2 Autoregulatory feedback loop
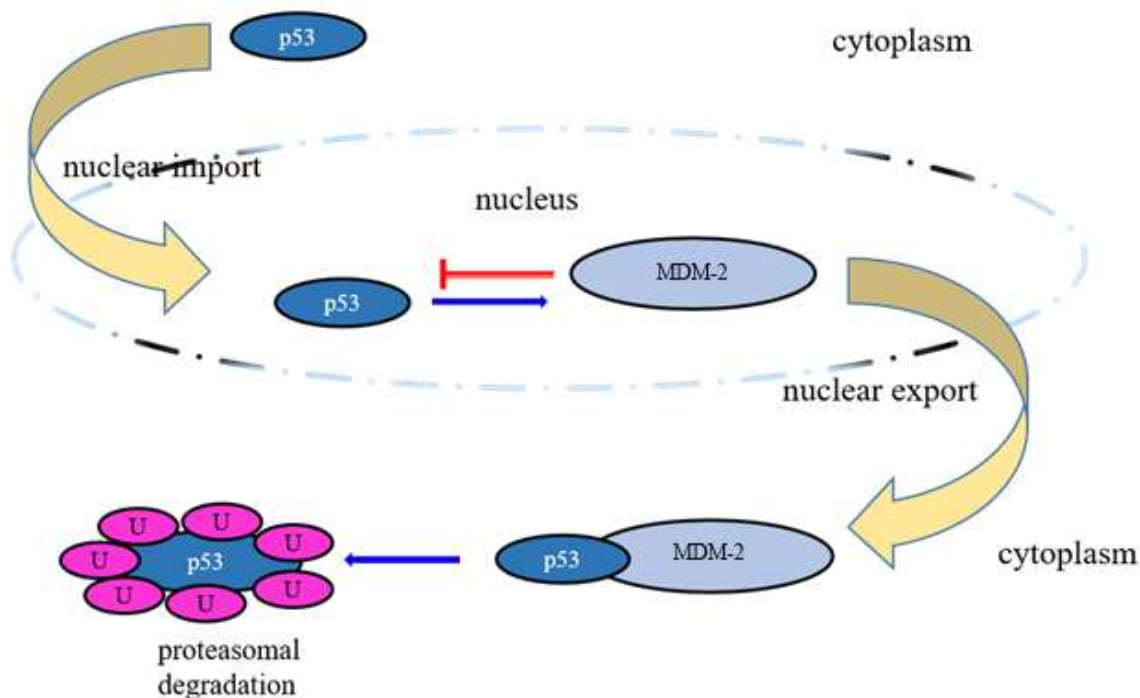
Figure 1.4.1. The negative autoregulatory feedback loop. *p53 regulates MDM2 expression by binding to its promoter. The MDM2, in turn, suppresses p53 by directly binding transcriptional activities, by binding at the p53 transactivational domain and by targeting p53 for proteasomal degradation. The autoregulatory feedback loop helps to keep low p53 protein level in normal cells.*

The MDM2 gene is either over-expressed or amplified in a significant number of human cancers (Momand et al., 1998). MDM2 is one of p53's transcriptional targets, and it is activated by p53 as the autoregulatory loop (Bond et al. 2005). Under normal physiological conditions, the p53 level is regulated by the MDM2 protein. In turn, the MDM2 protein directly binds to the N-terminal of the p53 protein and is targeted for protein degradation (Jones et al. 1995). It is not surprising that the MDM2 gene is either over-expressed or amplified in a significant number of human cancers (Momand et al., 1998).

1.5 Small molecule inhibitor – Nutlin3a
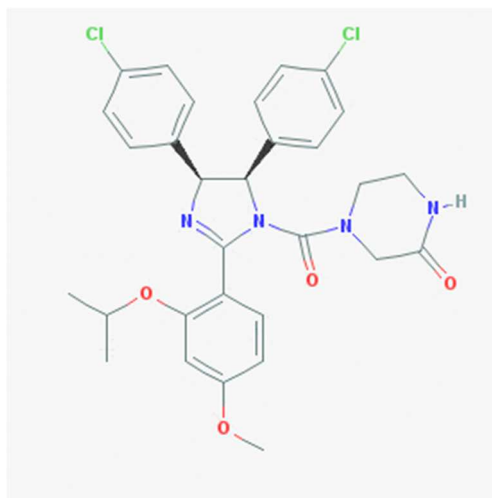
Figure 1.5.1. The chemical structure of Nutlin-3a *(Source PubChem)*

The crystal structure of MDM2 bound to the peptide of p53 transactivation domain revealed that MDM2 possesses a hydrophobic pocket (Vassilev et al. 2004). The presence of the pocket on the Mdm2 protein provided the hypothesis that compounds with low molecular weight could fit in the pocket to block the interaction of MDM2 with p53. A diverse library of synthetic chemicals was used to identify compounds for the pocket of MDM2 (Vassilev et al. 2004). The Nutley inhibitor (Nutlins) compound disturbed the binding of the recombinant p53 protein with MDM2 with inhibitory concentration (IC_{50}) values in the 100-300 nM range (Vassilev et al. 2004). The crystal structure of human MDM2-Nutlin2 complex confirmed that the inhibitor binds to the p53 binding site on MDM2 to a high degree, occupying all three binding pockets of MDM2 (Vassilev et al. 2004). Nutlin-3a has the potent binding activity and IC_{50} of 0.09 µM in comparison with the rest of its analogues (Vassilev et al. 2004). According to the model for p53 regulation by MDM2, treating cells with the inhibitor (Nutlin compound) resulted in (1)

stabilization and accumulation of p53 protein due to MDM2 inability to export p53 protein from nucleus to cytoplasm for protein degradation, (2) transactivation of MDM2 expression and (3) activation of p53 transcriptional activities (Vassilev et al. 2004). These molecular events in turn contribute to cell cycle arrest, apoptosis or both in cells with wild-type p53 (Vassilev et al. 2004). The wild-type p53 level increases in cells treated with the Nutlin compound as well as the level of MDM2 and p21, which is consistent with the activation of the p53 pathway (Vassilev et al. 2004). Nutlin-3, arbitrarily called enantiomer-a (Nutlin-3a), was used in many of the experiments as part of this thesis because it possesses potent binding activity in comparison with other enantiomers.

1.6 Forward genetic screening using a small molecule inhibitor

We employed a similar experimental approach that was originally used to identify RAS oncogene from a phage library. In the original approach that identified RAS oncogene from a phage library, DNA from human tumor cells was used to transfect mouse 3T3 cells and cultured for two weeks. The transformed cells were observed, and the DNA was extracted from those transformed cells to transfect mouse 3T3 cells for the second time. After the second round of transfection and the selection of the transformed phenotype, the phage library was constructed from the extracted DNA of the transformed 3T3 cells. By using a human-specific *Alu* probe, the phage library was screen for bacteriophages carrying human DNA. This forward genetic screening approach resulted in the identification of RAS oncogene (Parada et al. 1982) (PMID:6283357). We used similar approach with minor modification to identify candidate genes that negatively regulate wild-type p53 function. We used total RNA isolated from twelve

individual ovarian tumor tissue samples to create a pooled tumor-derived cDNA library. The

pooled patient-derived cDNA library was transduced into A2780 ovarian cancer cells with wild-

type p53. Using Nutlin-3a resistance as a phenotypic screening tool, we identified the candidate

exogenous negative effectors of p53 in these cells. The resistance to Nutlin-3a conferred by

exogenously transduced genes from the library suggests these candidate genes produce negative

effects on p53 activities related to apoptosis and cell cycle arrest.
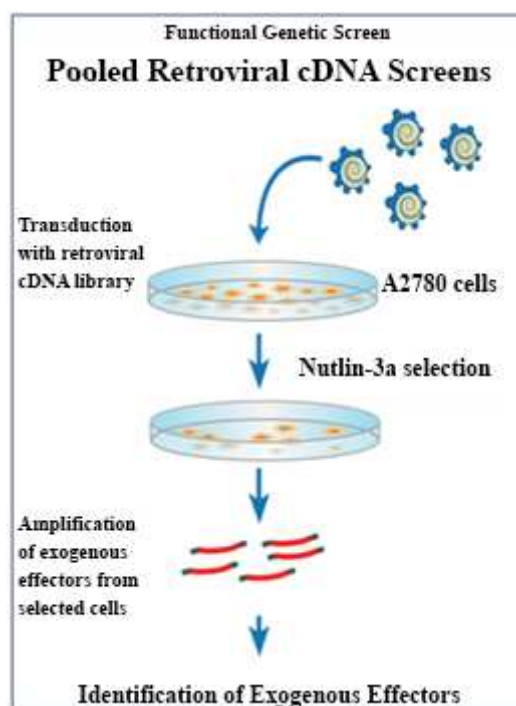
Figure 1.6.1. The concept of a forward genetic screening. *If there are surviving cells after the Nutlin-3a selection, those cells will have the exogenous effector or effectors that are negatively regulating the wild-type p53 protein functions.*

1.7 Specific aim

The primary goal of this thesis is to identify negative regulators of p53 function in ovarian cancers and to have a better understanding of p53-dependent transcriptional activities in ovarian cancer patients with wild-type TP53.

Chapter 2: Materials and Methods

2.1 The patient-derived pRetro-LIB cDNA library

The pRetro-LIB patient-derived cDNA library was constructed using in a total of twelve carcinoma samples from patients with ovarian cancer. These tumor samples were collected and used in accordance with approved protocol by the institutional review board of the Mayo Clinic. Most of the patients had primary advanced stage disease, while three recurrent tumor samples were also included in the total of 12 ovarian tumors. Ten out of 12 patients had the treatment-free interval (TFI) less than 6 months and were considered to have the chemotherapy-resistant disease. The TFI for two patients were not known. The tumors consist of the following subtypes of ovarian cancer: nine high-grade serous, two clear cell, and one endometrioid. Using Trizol RNA purification methods, the total RNA was extracted from nine primary and three recurrent ovarian tumors. The total RNA (2 μg) from each tumor sample was pooled together to generate a custom patient-derived retroviral cDNA library. The library was generated using a contract service from the Clontech Laboratories (Mountain View, CA).

2.2 Cell lines and cell culture

Human ovarian cancer cell line, A2780, was provided by Dr. Andrew Godwin (the University of Kansas Medical Center). A2780 cells are *TP53* wild-type and based on molecular profiling are speculated to be of clear cell origin (Domcke et al. 2013). Cancer cells were cultured in the media 1:1 mixture of M-199/MCDB-105 (catalog # M4530 and M6395) from Sigma-Aldrich (St. Louis, MO, USA) supplemented with 5% fetal bovine serum (catalog # F8067) from Sigma-Aldrich (St. Louis, MO, USA), and 1% penicillin and streptomycin (catalog # K952) from VWR (Radnor, PA, USA). The Phoenix-AMPHO cell line (catalog # STCC CRL-

3213) was purchased from ATCC. The Phoenix-AMPHO cells were maintained in high glucose Dulbecco's modified Eagle's medium (DMEM) media (catalog # D5796) from Sigma-Aldrich (St. Louis, MO, USA), supplemented with 10% fetal bovine serum (catalog # F8067) from Sigma-Aldrich (St. Louis, MO, USA) and 1% penicillin and streptomycin (catalog # K952) from VWR (Radnor, PA, USA) according to ATCC recommendation. All cells were maintained in a humidified atmosphere at 37°C with 5% CO_2/air atmosphere and passaged using 0.25% trypsin/EDTA (catalog # T4049) from Sigma-Aldrich (St. Louis, MO, USA).

2.3 Retroviral production

The helper plasmids VSV-G and gag-pol were used together with the patient-derived cDNA plasmid library to transfect Phoenix –AMPHO cells (catalog # ATCC CRL-3213) from ATCC (Manassas, VA, USA) for retroviral particles. Transfection was performed using the Lipofectamine LTX with PLUS reagent (catalog #15338030) from Invitrogen (Waltham, MA, USA) in OPTI-MEM media (catalog #11-058-021) from Invitrogen (Waltham, MA, USA). The empty plasmid was used as the control for transfecting Phoenix-AMPHO cells. After 5 hours post-transfection, the regular media was added into cells to a total volume of 10 mL. The transfected cells were cultured in a humidified atmosphere at 37°C with 5% CO_2/air atmosphere, and retroviral particles were harvested after 48 hours and 72 hours post-transfection. The collected retroviral particles were centrifuged at 2,000 rpm at 4°C for 10 min to remove the cell pellet. The supernatant was filtered through a syringe filter using 0.45 µM low protein binding membrane (Millipore steriflip HV/PVDF) to remove any trace of cell debris. After taking out the required amount of retroviral particle for titration with the kit, the rest of the aliquots were stored

at -80°C until future usage. The retroviral titer was determined by using Retro-X qRT-PCR Titration Kit (catalog# 631453) from Takara Bio USA (Mountain View, CA, USA) so that multiplicity of infection (MOI) of 1 could be calculated from the retroviral titer concentration. The filter retroviral particles were transduced into the ovarian cancer cells A2780 after the retroviral titer was determined by qRT-PCR Titration kit.

2.4 pRetro-cDNA library screening

Ten million A2780 cells were transduced with retroviral particles at a multiplicity of infection (MOI) of 1 in the media containing the infection reagent polybrene (4 µg/ml) (catalog #H9268) from Sigma-Aldrich (St. Louis, MO, USA). Nutlin-3a (40 µM) (catalog# S8059) from Selleckchem (Houston, TX, USA) was added to the A2780 cells after 24 hours of post-infection with retroviral particles. Nutlin-3a was added every 48 hours for three times with fresh media after washing with phosphate-buffered saline (PBS). The retroviral particles with empty plasmids were used as the control in A2780 cells during the library screening experiment. The surviving clones were picked up individually and transferred to one clone per well into 24-well plates. Those cells were re-plated into two 35-mm dishes, and the first well of the cell was used to extract gDNA to perform the pRetro-specific PCR to identify the potential candidate genes from the screen. The second well of the cells was kept for the culture for future experiments.

2.5 Genomic DNA (gDNA) extraction

The 5×10^6 cells were harvested by using trypsin treatment and the cell pellet from pRetro-cDNA-infected A2780 cells was collected. The cell pellet was washed twice with 1X

PBS and re-suspended in 500 µL of 1x PBS solution. The cell pellet was digested with protease

K solutions, lysed cells and extracted genomic DNA according to the manufacturer protocol. The

Blood & Cell Culture DNA Mini Kit (catalog # 13323) from Qiagen (Germantown, MD, USA)

was used to extract the genomic DNA of pRetro cDNA transfected A2780 cells.

2.6 pRetro-LIB-specific PCR

The PCR reaction was performed using the patient-derived pool cDNA library specific

primers called pRetro-LIB primers. Amplification was performed in 50 µL reaction volume and

consisting of 10.0 µL nuclease-free water, 2.50µL forward primer (300 nM), 5.0 µL reverse

primer (300 nM), 5.0 µL of Expand High Fidelity buffer (5X), 1.0 µL of template (250 ng), 0.75

µL of Expand Long Taq polymerase mix (catalog # 04 738 268 001) from Roche (Indianapolis,

IN, USA) and 1.0 µL of dNTP mix (200 µM). PCR was performed using the Bio-Rad T100

Thermal Cycler machine. The thermal cycle was programmed for 2 minutes at 94°C for initial

denaturation, 10 cycles of PCR reaction with each cycle constituting 30 seconds at 94°C for

denaturation, 30 seconds at 56.5°C for annealing, 8 minutes at 68°C for extension, and followed

by an additional 25 cycles of PCR reaction with each cycle constituting 30 seconds at 94°C, 30

seconds at 56.5°C, 8 minutes with 20 second increment per cycle at 68°C and 10 minutes at 68°C

for final extension. PCR products were examined by electrophoresis at 180V for 30 minutes in a

1% (w/v) agarose gel in 1X TAE buffer. The 1kb DNA ladder (catalog # N3232L) from New

England Biolabs (Ipswich, MA, USA) was used as the marker. The EZ-Vision One (catalog #

97064-192) from VWR (Radnor, PA, USA) was added into electrophoresis gel solution for

visualization of the PCR products. The PCR products were visualized and documented using the ChemiDoc ^{TM} MP Imaging System (BioRad). The primer sequences are listed in Table 2.6.1.

PCR		
Primer Name	Forward Sequence	Reverse Sequence
pRetro-LIB	5'-AGCCCTCACTCCTTCTCTAG-3'	5'-ACCTACAGGTGGGGTCTTTCATTCCC-3'

Table 2.6.1. *Lists of primer sequences used in pRetro-LIB specific PCR reaction.*

2.7 Antibodies and compound

Mouse monoclonal anti-NIFK (18E148) antibody (catalog # sc-52904) and mouse monoclonal anti-p53 (DO1) antibody (catalog# sc-126) were purchased from Santa Cruz Biotechnology (Sant Cruz, CA, USA). Mouse monoclonal anti-NIFK (18E148) antibody (catalog # GTX13880) was purchased from GeneTex (Irvine, CA, USA). Mouse monoclonal anti-NIFK (CL2240) antibody (catalog # ab211871) was purchased from Abcam (Cambridge, MA, USA). Mouse monoclonal anti-beta-actin antibody (catalog# A1978) was purchased from Sigma-Aldrich (St. Louis, MO, USA). For secondary antibodies, anti-mouse IgG-HRP antibody (catalog # sc-2371) was purchased from Santa Cruz Biotechnology (Santa Cruz, CA, USA). Nutlin-3a (catalog# S8059) was purchased from Selleckchem (TX, USA). Nutlin-3a solutions were dissolved in DMSO (catalog #) at 100mM and stored at -80°C.

2.8 Immunoblotting

Cells were scraped and centrifuged at 1,000 xg for 5 minutes to get the cell pellets. The cell pellets were washed with 1X ice-cold PBS solution twice and lysed in 2X Laemmli sample

buffer (catalog # 161-0737) from Bio-Rad Laboratories (CA, USA) with 5% β-mercaptoethanol (catalog # M3148-100mL) from Sigma-Aldrich (St. Louis, MO, USA). The cell lysates were boiled at -95°C for 5 minutes before being loading into SDS polyacrylamide gel.

2.9 Real-time quantitative PCR (RT-qPCR)

The total RNA was extracted with the Trizol reagent (catalog # 15-596-018) from Invitrogen (Waltham, MA, USA) according to the manufacturer's protocol. One µg of total RNA was used for cDNA synthesis using SuperScript II reverse transcriptase (catalog # 18064-014) from Invitrogen (Waltham, MA, USA) according to the manufacturer's protocol in a 20 µL reaction. The cDNA was diluted into 1:20 in nuclease-free water and 1 µL of diluted cDNA was used in the qPCR reaction with triplicates. The RT SYBR Green Flour qPCR Master Mix (catalog # 330513) from Qiagen (Germantown, MD, USA) was used in the reactions. The CFX384 Real-Time PCR Detection System (Bio-Rad) was used to perform the qPCR reactions. In addition, the non-template negative control was included in the qPCR reaction. The 18S rRNA was used as the amplification control to normalize the level of mRNA expression. The sequences of the primers were listed in Table 2.9.1.

qRT-PCR		
Primer Name	**Forward Sequence**	**Reverse Sequence**
Mdm2	5'-TGCCAAGCTTCTCTGTGAAAG-3'	5'-TCCTTTTGATCACTCCCACC-3'
GADD45	5'-GGAGAGCAGAAGACCGAAAG-3'	5'-AGGCACAACACCACGTTATC-3'
p21	5'-ATGAAATTCACCCCCTTTCC-3'	5'-CCCTAGGCTGTGCTCACTTC-3'
p53	5'-GTCCCAAGCAATGGATGATTT-3'	5'-GTTGTAGTGGATGGTGGTACAG-3'
18S	5'-GCCCGAAGCGTTTACTTTGA-3'	5'-TCCATTATTCCTAGCTGCGGTATC-3'

Table 2.9.1. *Lists of primer sequences used in quantitative reverse transcriptase polymerase chain reaction (qRT-PCR)*

2.10 siRNA transfection

A2780, A2780-NIFK, A2780-ΔKiFHA, A2708-ΔRRM and, A2780-T234/8-A cells were seeded in 6-well plates (0.35 x 10^6 cells per well). Both control and MDM2 siRNA were purchased from IDT (Coralville, IA, USA). Lipofectamine 2000 reagent (catalog # 11668-019) was purchased from Invitrogen (Carlsbad, CA, USA). The siRNAs and transfection reagent were added into the OPTI-MEM medium (catalog #51985091) from Invitrogen (Carlsbad, CA, USA) and incubated for 5 minutes at room temperature. The cells were washed with 1X PBS solution, and fresh Opti-MEM and siRNAs transfection mixture were added to the cells. Nutlin-3a (40 μM) in M-199/105 media was added after 48 hours of post-transfection after the cells were washed with 1X PBS solution. After 24 hours later, cells were harvested and collected for the experiments.

2.11 Clonogenic assay

A2780, A2780-NIFK, A2780-ΔKiFHA, A2708-ΔRRM and, A2780-T234/8-A, 500 cells were seeded in 6-well plates to measure the proliferation. Cells were treated with different concentrations of Nutlin-3a (10 µM, 20 µM, 30 µM and 40 µM) and incubated for 72 hrs. The cells were washed with 1X PBS once before adding the fresh media after 3 days with Nutlin-3a treatment. The fresh media were added every 3 days after 1X PBS wash, and the colonies were allowed to form up to 14 days. At the end of the experiment, the cells were stained with Crystal Violet (catalog # C0775-110G, Sigma-Aldrich, St. Louis, MO, USA) Fixing/Staining solutions.

Chapter 3: Results

3.1 Results

3.1.1 Patient-derived cDNA library is used to identify negative regulators of the p53 pathway in ovarian cancer with wild-type p53 by a forward genetic screen.

To identify the potential negative regulators of the p53 pathway, we used Nutlin-3a as the tool to induce p53 pathway in ovarian cancer cells with wild-type p53. The total RNA from 12 ovarian carcinoma samples was extracted, and the cDNA was generated using reverse transcriptase enzyme. The summary of tumor information is listed in Table 3.1.1. We also sequenced the selected tumor samples from the patient-derived pool cDNA library to make sure that the reference transcripts were present in our library using Next Generation Sequencing (NGS) technology from Illumina (Table 3.1.2). The data from the MiSeq sequencing of the cDNA library and GAII sequencing of the select tumor samples suggested a decrease in representation of novel transcripts and splice variants in the cDNA library. This decrease in presentation may be related to lower transcript coverage resulting from a reduced sequencing output from the MiSeq sequencing.

Patient-derived cDNA library

OV#	Histology	Type	Grade	Stage	TFI
527	Serous	Primary	4	4	0
536	Serous	Recurrent	3	3C	2.4
656	Serous	Primary	4	3C	0
687	Clear cell	Primary	3	3C	0
844	Serous	Primary	3	3C	0
988	Serous	Primary	4	3C	1.9
991	Clear cell	Primary	3	3C	
1024	Serous	Primary	4	3C	3.4
1061	Serous	Recurrent	4	2C	0
1070	Serous	Recurrent	4	3C	1
1120	Serous	Primary	4	3C	
1272	Endometrioid	Primary	3	3C	0.1

- mRNA → cDNA → retroviral cDNA library
- 10^{10} cfu/ml in the library
- 3×10^6 independent clones in the library
- 93% of the clones have inserts
- Average size is 1.69 kb (0.8-3.5 kb)

Table 3.1.1 Tumor types, histology, grade and stages of tumors in patient-derived cDNA library. Total RNA from individual patients' tumors was extracted, pooled, and used to construct a retroviral-based cDNA library that was then transduced into A2780 cells.

| Sample | Annotated Trascripts | New Transcripts | | Total Transcripts | # of mapped reads |
		Splicing variants	Novel transcripts		
cDNA library MiSeq	10838	808	1657	13303	11,075,394
Tumor 1	20129	3977	16708	40814	42,598,377
Tumor 2	20138	3844	17132	41114	42,919,650
Tumor 3	20018	3831	16708	40557	44,823,659
Tumor 4	21435	3843	13107	38385	40,783,093
Tumor 5	20832	3324	15177	39333	39,117,804
Tumor 6	21433	3958	19541	44932	41,445,359
Tumor 7	21443	3788	15877	41108	35,908,079

Table 3.1.2 *The patient-derived pool cDNA library and selected patients' tumor samples were sequenced using Next Generation Sequencing by Illumina. The sequencing result proved that there were transcripts in both the library and tumor samples.*

3.1.2 Proof of concepts of screening procedure in target cells (A2780)

We performed the different infection methods to compare the transduction efficiency of retroviral cDNA library in A2780 cells. As a control, we used the pRetro-mCherry to visualize transduction efficiency in A2780 cells. We used 90% of the cDNA library and 10% of pRetro-mCherry in Phoenix-AMPHO cells to produce the retroviral particles. We used two different cell lines, A2780 and NCI-H23, to transduce them with retroviral particles. From the results, the spin-fection method produced higher transduction rate in both cell lines (Figure 3.1.2). Therefore, we used the spin-fection methods in subsequent studies to transduce A2780 cells with the retroviral particles from the cDNA library.

To establish MOI for the infection experiment using the retroviral particles from the patient-derived cDNA library, we performed the qRT-PCR titration using the Retro-X qRT-PCR kit (catalog # 631453) from Clontech (Mountain View, CA, USA). We used the NucleoSpin RNA Virus Kit (catalog # 740956) from Clontech (Mountain View, CA, USA) to isolate viral RNA from the supernatant using the manufactory's recommended methods. We followed the user manual without modification. The RNA copy number was tested with the filtered retroviral particles after 48 hours of post-infection to determine the multiplicity of infection (MOI) number for the infection experiment in the target cells. From the qRT-PCR result, the retroviral titer of the patient-derived cDNA library was 9.23 x10^8 copy/mL (Figure 3.1.1).
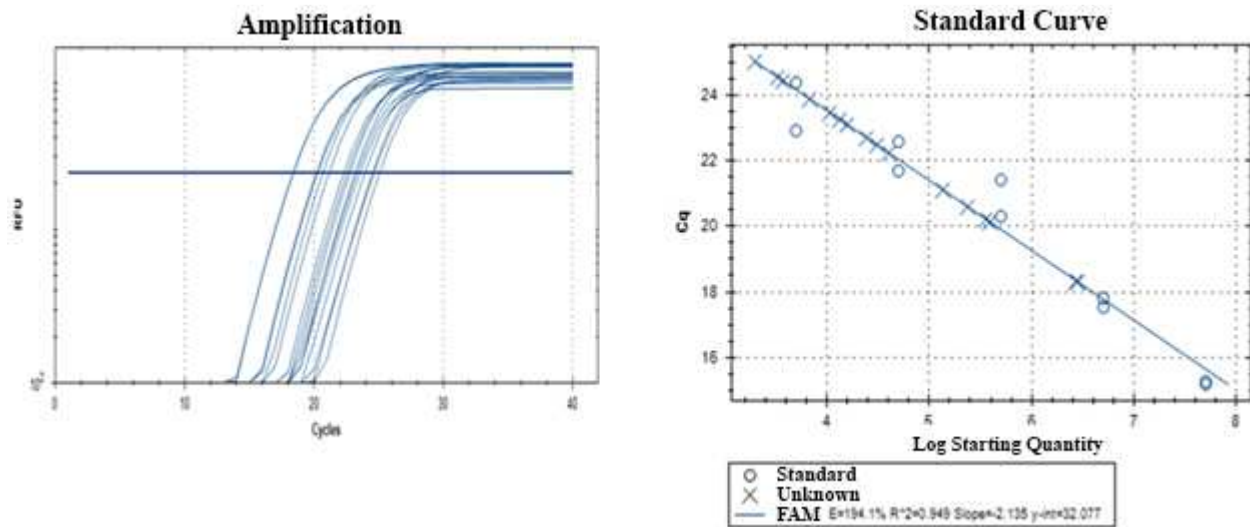
Figure 3.1.1 The concentration of viral particles was determined using the Retro-X qRT-PCR kit. *The viral particles were collected after 48 hours or 72 hours of post-infection and subjected to test for RNA copy number using Retro-X qRT-PCR Titration Kit.*

We initially planned to use MOI of 1 for the infection experiment in A2780 cells. However, due to the very low transduction efficiency in A2780 cells, we ended up using MOI of 2 for our infection experiment. From the results, the spin-fection method proved to have higher transduction rate in both cell lines (Figure 3.1.2).

A2780

NCI-H23

Regular method   Spin-fection method
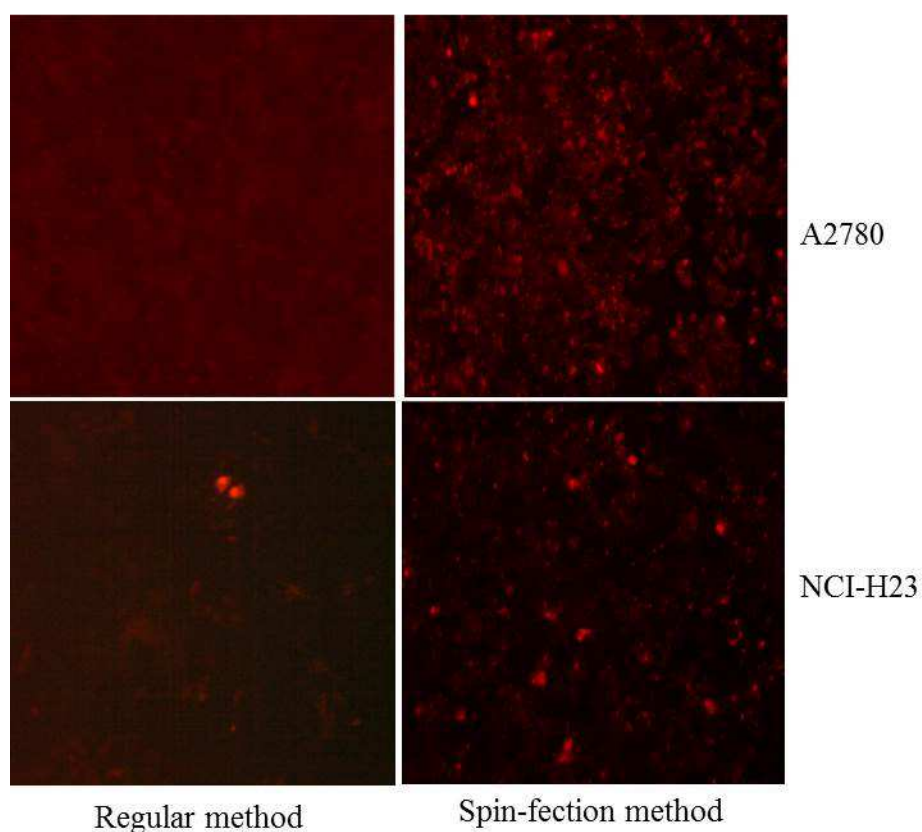
Figure 3.1.2 The proof of concept of the experimental methods and design. *A2780 and NCI-H23 cells were transduced with retroviral particles of pool cDNA library together with 10% of retroviral particles of mCherry. The fluorescence signals from pRetro-mCherry were observed in the cells.*

3.1.3 The different concentration of Nutlin-3a to be used in a forward genetic screen is tested.

We then tested the concentration of Nutlin-3a that is sufficient to suppress the clonogenic growth in A2780 cells. A2780 cells (cell number 5 x 10^6) were seeded in 150-mm tissue culture plate for overnight. The next day, different concentrations of Nutlin-3a (20, 40, 60, 80 and 100 µM) were added to the fresh culture media every 24 hours up to three times. The media was discarded after 24 hours of the last treatment and washed with 1X PBS solution twice. The fresh regular culture media was added, and the cells were allowed to grow for another 14 days. The fresh media was added to the plates every 3 days after washing with 1X PBS solution. The result indicated that 40 µM Nutlin-3a was the best concentration to use in the screening experiment due to the one surviving clone in A2780 cells (Figure 3.1.3) to rule out the false positive result in screening experiment.
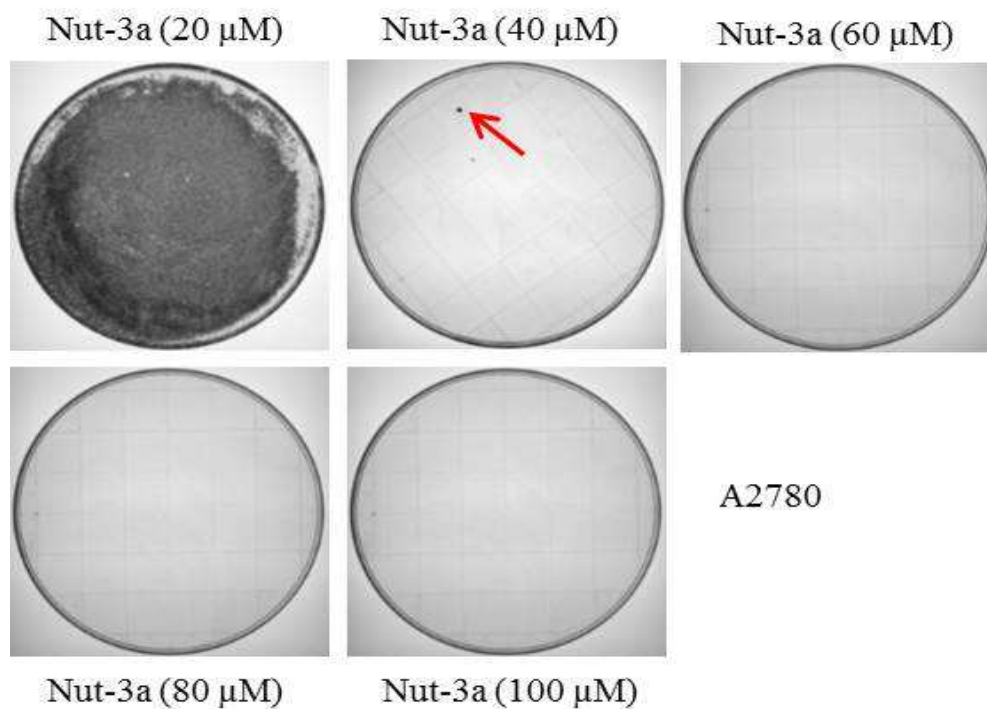
Figure 3.1.3 Nutlin-3a shows decreased in the survival of A2780 cells with increasing concentration. *The ovarian cancer cells (A2780) were treated with different concentrations of Nutlin-3a ranging up to 100 μM in 150-mm plates three times. The surviving cells were cultured for 14 days after the last dose of Nutlin-3a. The result indicated that 40 μM Nutlin-3a selection is appropriate for selection to limit false positives.*

3.1.4 pRetro-LIB vector-specific PCR is used to identify the candidate negative regulators of the p53 pathway in the screening.

We used the vector-specific primers listed in Table 2.1.1 to rescue and identify exogenously transduced genes in surviving colonies after Nutlin-3a selection. We used the purified plasmid from the patient-derived pool cDNA library (henceforth referred to as pRetro-LIB unless otherwise stated) as our positive control and genomic DNA of A2780 as our negative control in PCR reaction. Initially, we extracted genomic DNA from parental A2780 cells and from the cDNA library-infected cells, using the Blood & Cell Culture DNA Mini Kit (catalog #13323) from Qiagen (Germantown, MD, USA). The PCR reaction was performed using Expand High Fidelity PCR system (catalog # 04 738 250 001) from Roche (Indianapolis, IN, USA) in 50 µL reaction. The PCR products were run on 0.7% agarose gel to verify the product size. From the result on the agarose gel (Figure 3.1.4), we observed a similar smear pattern for all pRetro-LIB library including from A2780 cells infected with the patient-derived cDNA library. Only genomic DNA of A2780 cells did not have the smear pattern as expected.
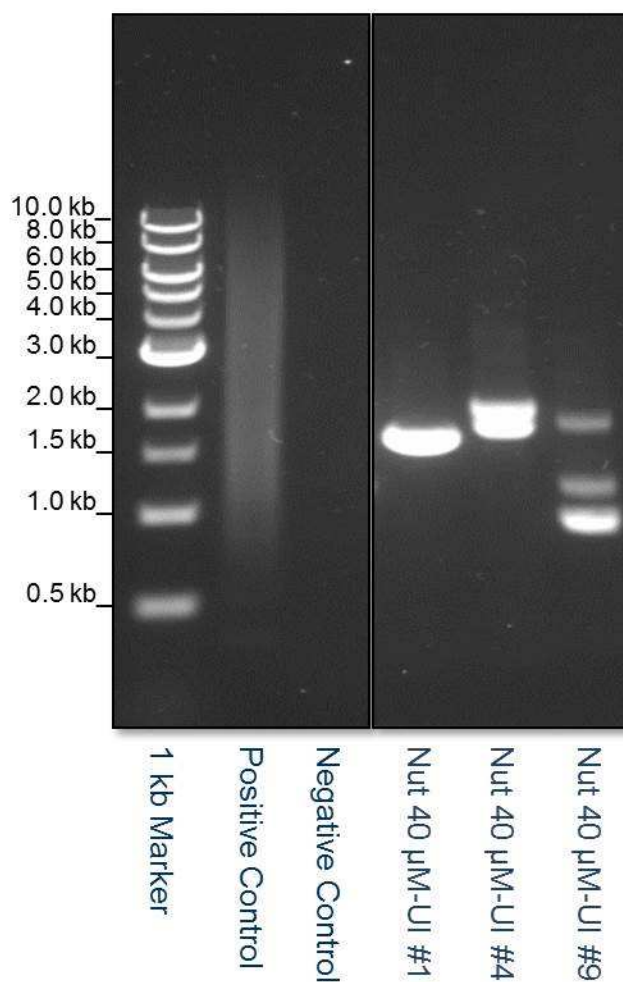
Figure 3.1.4 The PCR products of patient-derived cDNA library. *Genomic DNA isolated from either parental A2780 and A2780 cells infected with patient-derived pool cDNA library were amplified by PCR using pRetro library specific primers and the produces run on an agarose gel. The positive control is the genomic DNA of pRetro-LIB plasmid and the negative control is genomic DNA of A2780 cells. The genomic DNA of Nutlin-3a produced clones were subjected to PCR and run on the agrose gel.*

3.1.5 Exogenous effector or effectors are identified from functional genetic screening.

The selection of the library-infected cells with 40 µM Nutlin-3a produced fifteen surviving colonies. We randomly picked up three colonies to extract genomic (gDNA) and

performed Sanger sequencing on the PCR products to identify potential candidate exogenous effectors. The main reason to pick up only three colonies were due to the time limitation and the genomic (gDNA) from the rest of the colonies were extract for the future use. The Sanger sequencing identified three candidate cDNAs, *i.e.,* NIFK, GXYLT 1, and SACS, which encode for proteins that can putatively act as negative regulators of p53 function. Based on the sequencing results from four independent screening experiments, NIFK was the one candidate that showed up in all clones selected. NIFK is also known as Nucleolar Protein Interacting with the FHA Domain of MKI67 (MKI67IP) and nucleolar phosphoprotein (Nopp34). It is a putative RNA-binding protein and was discovered in the yeast two-hybrid screening using Ki-67 FHA domain as the bait (Takagi et al. 2001), and was also confirmed by directed proteomics analysis (Andersen et al. 2002). NIFK protein interacts with Ki-67 through its FHA domain and the function of human NIFK protein in cancer is unknown (Li et al. 2004). In general, NIFK protein consists of 293 amino acids and contains a N-terminal RNA recognition motif (RRM), a Ki-67 FHA binding domain, and a lysine-rich domain (Li et al. 2004). Two phosphorylation sites, Thr^{234} and Thr^{238} of NIFK, were shown to be required for the interaction between NIFK and Ki-67 FHA domain (Takagi et al. 2001). The binding between the Ki-67 FHA domain and NIFK appears to require a longer peptide fragment of 44 amino acid residues in vitro experiments (Li et al. 2004). The RNA recognition motif (RRM) of NIFK protein is probably required for cell cycle progression and ribosome biogenesis (Lin et al. 2016). The NIFK protein is known to localize mainly to nucleoli but has been detected in lower levels in the nucleoplasm and cytoplasm of cells. In previous studies, the nucleolar staining was reported to be reduced after the RNase A treatment prior to fixation in cells (Li et al. 2004) (Takagi et al. 2001).

NIFK Protein Structure
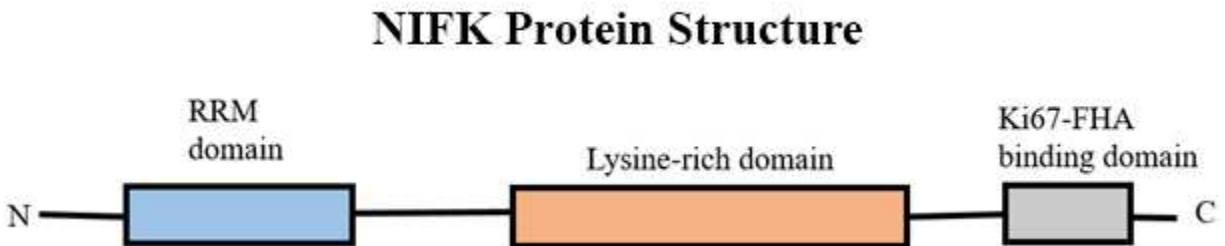
Figure 3.1.5*. Schematic diagram of NIFK protein structure. NIFK interacts with Ki-67 FHA domain and contains RNA recognition motif (RRM) and lysine-rich domain.*

3.1.6 NIFK overexpression in A2780 cells promotes resistance to Nutlin-3a in the proliferation assay.

Ki-67 is the nuclear protein that plays a role in cell proliferation, has high expression in diving cells in cell cycle, and is down-regulated in G_0 quiescent cells (Gerdes et al. 1984) (Verheijen et al. 1989). It is typically a cellular marker for proliferation, but the mechanism of Ki-67 in cancer is not well studied. In addition, previous studies have shown that very low-level of Ki-67 can co-localized with the RNA polymerase I (Pol I) transcription machinery and can physically interact with the promoter region of the chromatin of rDNA (Bullwinkel et al. 2006). Ki-67 involvement in cell cycles with other protein is possibly through FHA domain and Ki-67 FHA domain interacts with two novel proteins Hklp2 (human kinesin-like protein 2) and NIFK (human nucleolar protein interacting with the FHA domain of Ki-67) (Takagi et al. 2001) in a yeast two-hybrid screening. Thus, it is speculated that both proteins might play a role in signal transduction pathways in mammalian cells.

To explore the potential role of NIFK in cancer, we introduced four different GFP-tagged NIFK expression plasmids (kindly provided by Dr.Tsung-Chieh Lin, Genomics Research Center, Academia Sinica, Taipei, Taiwan) into A2780 cells using retroviral particles to generate cells that exogenously overexpresses NIFK. GFP-tagged NIFK expression plasmids (1) full-length NIFK (2) ΔKi-FHA; FHA domain of NIFK protein is deleted (3) ΔRRM; RNA recognition motif of NIFK is deleted (4) T>A; two phosphorylation sites Thr^{234} and Thr^{238} mutated to Alanine were used to investigate the molecular function of NIFK protein in ovarian cancer (Li et al. 2004). The NIFK overexpressing A2780 cells (cell number = 500) were seeded in 6-well plates and incubated overnight. Different concentrations of Nutlin-3a (10, 20, and 30 μM) were added to the cells. Vehicle (DMSO) treated cells were used as the control. We observed differences in the number of colonies formed when comparing parental A2780 cells and NIFK overexpression cells (Figure 3.1.6 A & B) (Figure 3.1.6 C). The difference in colony formation between parental and NIFK overexpression cells was most obvious in cells treated with highest concentrations of Nutlin-3a (30 μM).
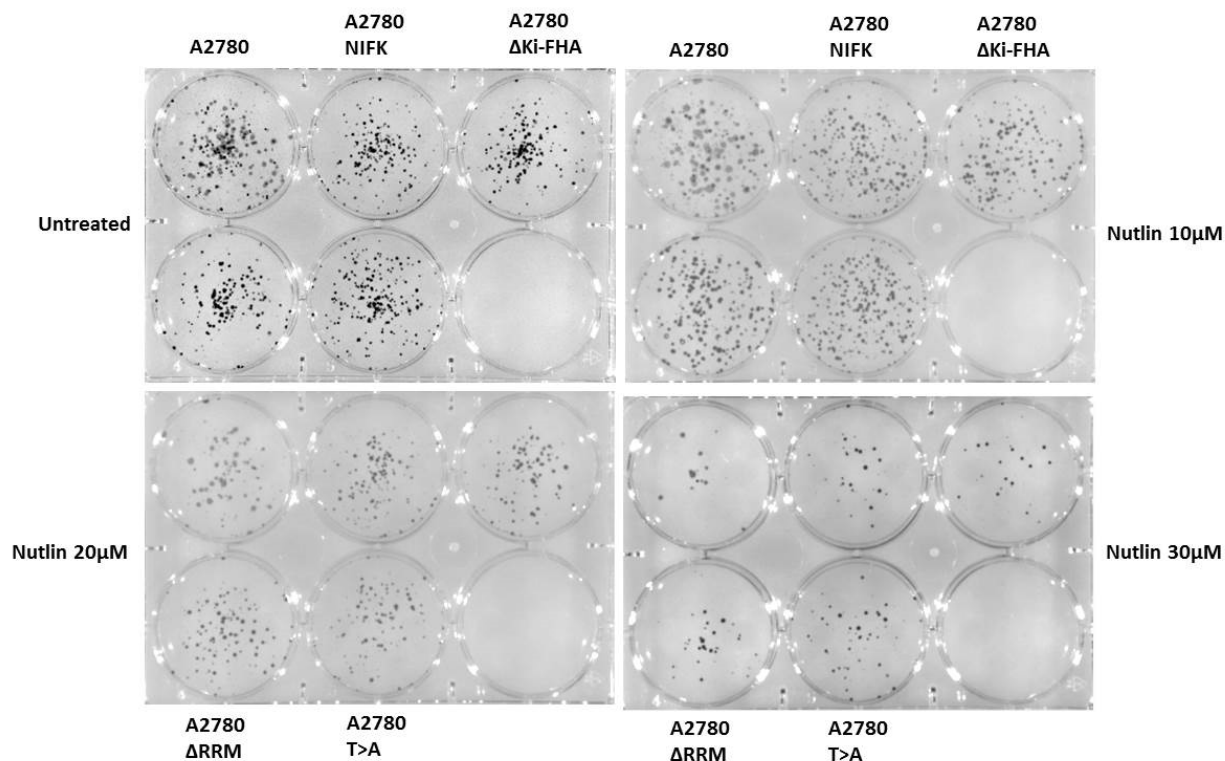
Figure 3.1.6(A & B) Colony Formation Assay. *A2780 cells were used for the overexpression of NIFK, NIFK ΔKi-FHA, NIFK ΔRRM and NIFK T>A. The NIFK overexpression cells and A2780 were plated in 6-well tissue culture plate for colony formation assay. Colony formation of A2780 cells was inhibited more as the concentration of Nutlin-3a increased. The NIFK overexpression cells were still forming colony even in high concentrations of Nutlin-3a compared to the A2780 cell.*
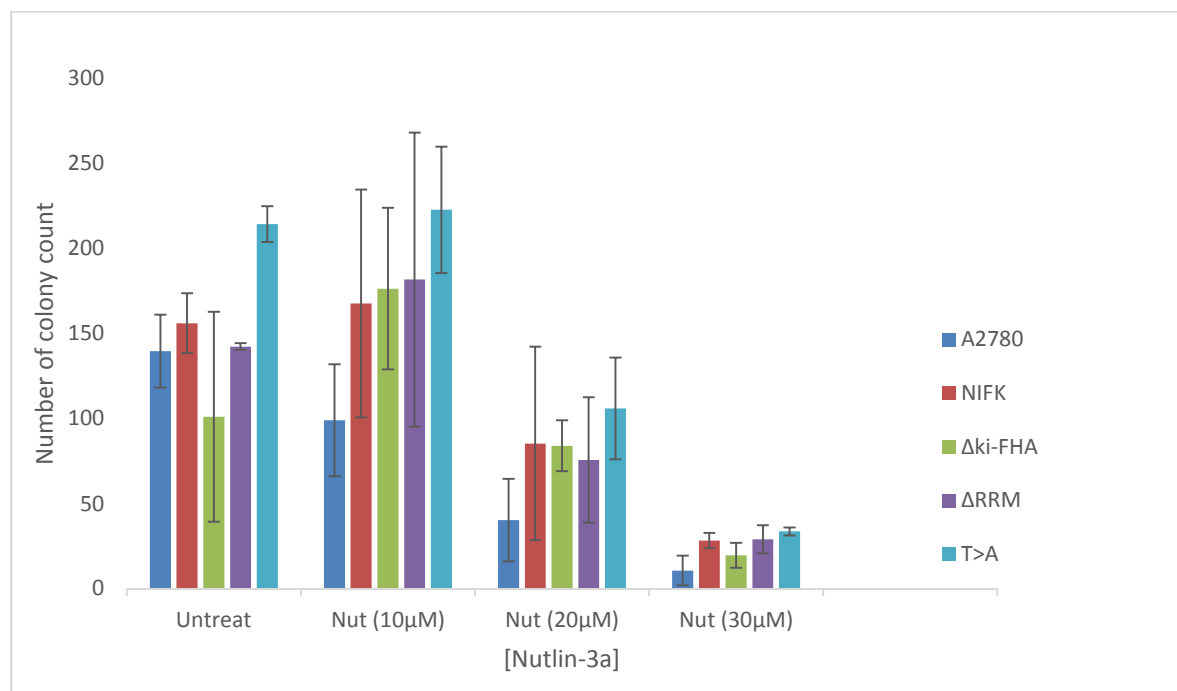
Figure 3.1.6(C) Colony Formation Assay. *The quantitation of colony formation of parental A2780 and cells overexpressing NIFK, NIFK ΔKi-FHA, NIFK ΔRRM and NIFK T>A.*

We tested the level of exogenous NIFK expression by Westen blots in A2780 and NIFK overexpression cells. Cells were either treated with Nutlin-3a (30 µM) or DMSO as the control and incubated overnight. Cell lysates were collected and subjected to Western blot using NIFK monoclonal antibody. The exogenous NIFK protein levels in (1) full-length NIFK (2) ΔKi-FHA; FHA domain of NIFK protein is deleted (3) ΔRRM; RNA recognition motif of NIFK is deleted (4) T>A; two phosphorylation sites Thr234 and Thr238 were changed to Alanine and were elevated after Nutlin-3a treatment (40 µM) compared with A2780 and control (DMSO) cells (Figure 3.1.6 D). We also tested other ovarian cancer cell lines for NIFK expression level and moderate to higher expressions were observed (data not included). To our surprise, the changes in exogenous level of NIFK expressions were not observed in lower concentration of Nutlin-3a

treatment such as 10 μM concentration (data not showed). Interestingly, the exogenous NIFK expression is upregulated after Nutlin-3a treatment compared with untreated control only in NIFK overexpression cells but not in A2780. One possible explanation for higher expression of exogenous NIFK in cells was due to differences in promoters. While endogenous promoter may be regulated by p53 and subjected to p53-mediated suppression, exogenous CMV promoter is not regulated by p53 in similar manner. The fact that exogenous NIFK expression is apparent only after endogenous NIFK expression was downregulated by Nutlin-3a suggests the levels of NIFK are tightly controlled in these cells. We also checked the expression of p53 and other proteins in its network such as p21, PUMA, and GADD45 (Figure 3.1.6 D). Consistent with the activation of p53 pathway by Nutlin-3a, we observed the induction of p21 and MDM2 and the suppression of c-Myc in Nutlin-3a-treated cells. PUMA expression is barely detectable in these cells and its expression is minimally increased in Nultin-3a-treated cells. The level of the growth arrest and DNA damage (GADD45) should have been induced upon Nutlin-3a treatment but the opposite effect was observed compare with untreated (DMSO) cells (Figure 3.1.6 D). However, GADD45 expression levels in A2780 and NIFK overexpression cells were almost the same in the Western blot regardless of treatment or control (Figure 3.1.6 D). Next, we examined the mRNA level of those genes by qRT-PCR to confirm that what we observed in protein level was also correlated with mRNA level (Figure 3.1.6 E). We observed that the mRNA expression of these target genes was increased by Nutlin-3a treatment compared with untreated (DMSO) (Figure 3.1.6 E). As expected, p53 could not regulate MDM2 transcription level upon Nutlin-3a treatment (Figure 3.1.6 E). The transcription levels of p53 were almost the same in Nutlin-3a treatment and untreated (DMSO) cells (Figure 3.1.6 E) but p53 protein levels in A2788 and

NIFK overexpression cells were higher in Nultlin-3a treatment (Figure 3.1.6 D). Interestingly, although the mRNA expression of GADD45 was induced by Nutlin-3a, the protein expression was decreased by Nultin-3a (Figure 3.1.6 D and Figure 3.1.6 E). These data suggest that future experiments will be required to identify why GADD45 protein level was decreased even though there was evidence that the transcription of GADD45 was induced by Nutlin-3a treatment. It might also be possible that NIFK protein plays a role to regulate the translation of GADD45 and that future experiments are required to identify the interaction of those two proteins.
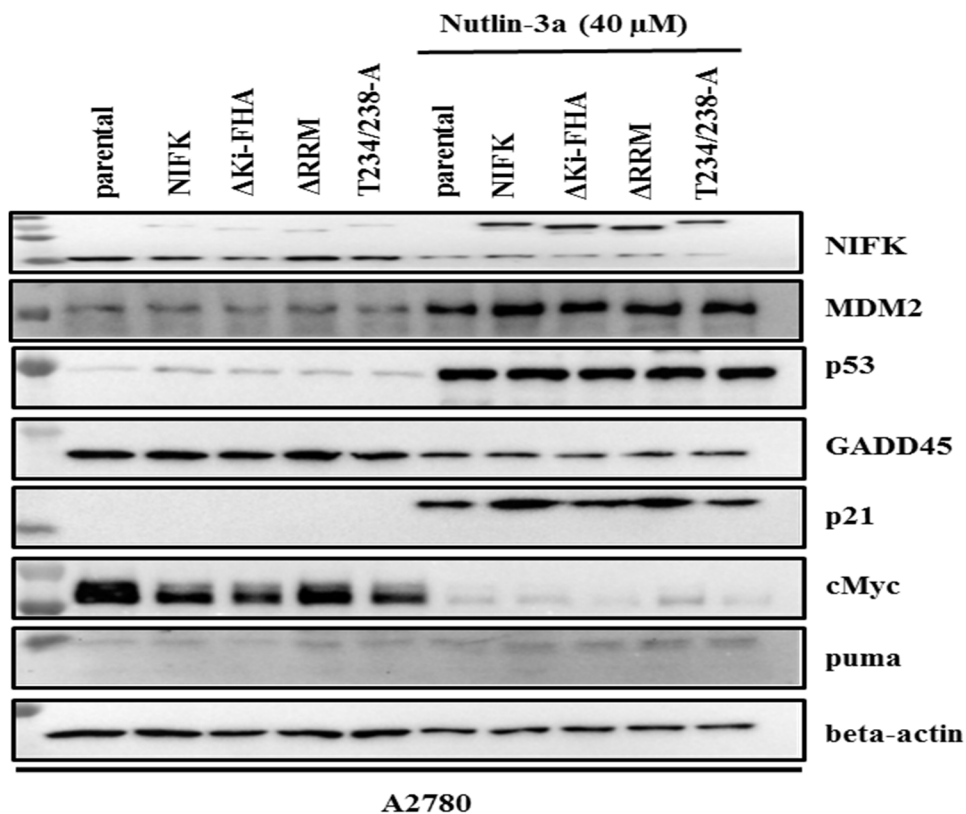
Figure 3.1.6 (D) Western Blot. *A2780 cells and the NIFK overexpression cells were either treated with DMSO or Nutlin-3a (40 µM) for 24 hours. Whole cell lysates were collected from the various cell lines and were subjected to immunoblotting with different antibodies. The ß-actin blot served as the loading control for all samples.*
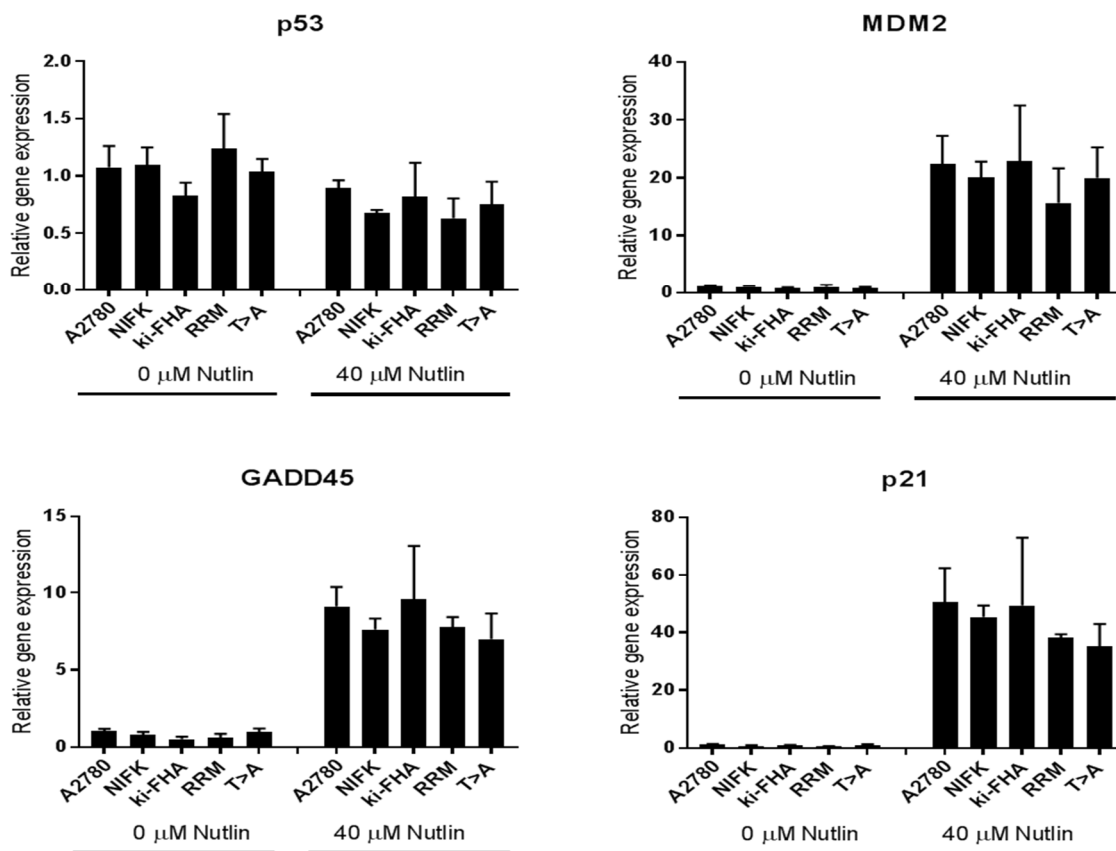
Figure 3.1.6 (E) qRT-PCR. *A2780 cells and the NIFK overexpression cells were either treated with DMSO (vehicle) or Nutlin-3a (40 µM) for 24 hours. The RNA was reverse-transcribed into cDNA and evaluation by qPCR to measure the transcript levels of various genes in the p53 networks.*

<div align="center">**qRT-PCR**</div>

Primer Name	Forward Sequence	Reverse Sequence
MDM2	5'-TGCCAAGCTTCTCTGTGAAAG-3'	5'-TCCTTTTGATCACTCCCACC-3'
GADD45	5'-GGAGAGCAGAAGACCGAAAG-3'	5'-AGGCACAACACCACGTTATC-3'
p21	5'-ATGAAATTCACCCCCTTTCC-3'	5'-CCCTAGGCTGTGCTCACTTC-3'
p53	5'-GTCCCAAGCAATGGATGATTT-3'	5'-GTTGTAGTGGATGGTGGTACAG-3'
18S	5'-GCCCGAAGCGTTTACTTTGA-3'	5'-TCCATTATTCCTAGCTGCGGTATC-3'

Table 3.1.3. *Lists of primer sequences used in quantitative reverse transcriptase polymerase chain reaction (qRT-PCR).*

MDM2 is an E3 ubiquitin ligase, and our observation that endogenous NIFK expression decreases upon MDM2 induction by Nutlin-3a (Figure 3.1.6 D) raises a possibility that NIFK expression may be regulated by MDMD2. To test this possibility, we used siRNAs to knock down *MDM2* expression in cells. Cells were plated in 6-well plates for siRNA experiments. After 48 hours post infection with control siRNA or MDM2 siRNA, Nutlin-3a (10 µM) in fresh media was added to the cells. Following an additional 24 hours, cells were harvested and subjected to Western blot analysis. The endogenous NIFK levels were increased in cells transfected with MDM2 siRNA compared to the cells transfected with the control siRNA (Figure 3.1.6 F). In untreated cells, the exogenous NIFK protein level was slightly increased in MDM2 siRNA compare to control siRNA (Figure 3.1.6 F). In Nultin-3a treated cells, the exogenous NIFK expression level was decreased in MDM2 siRNA (Figure 3.1.6 F). It is possible that NIFK regulates MDM2 and the route of regulation is needed to explore in ovarian cancer. The p53 and p21 protein levels were relatively remain unchanged but the slight decreased expression

were observed in full length NIFK expression Nutlin-3a treated cells upon MDM2 siRNA knockdown (Figure 3.1.6 F). There was the change in p21 protein levels in NIFK-ΔRRM overexpression cells after MDM2 siRNA knockdown in Nutlin-3a treatment (Figure 3.1.6 F). In addition, future experiments are needed to investigate the mechanism of NIFK in ovarian cancer with wild-type p53.
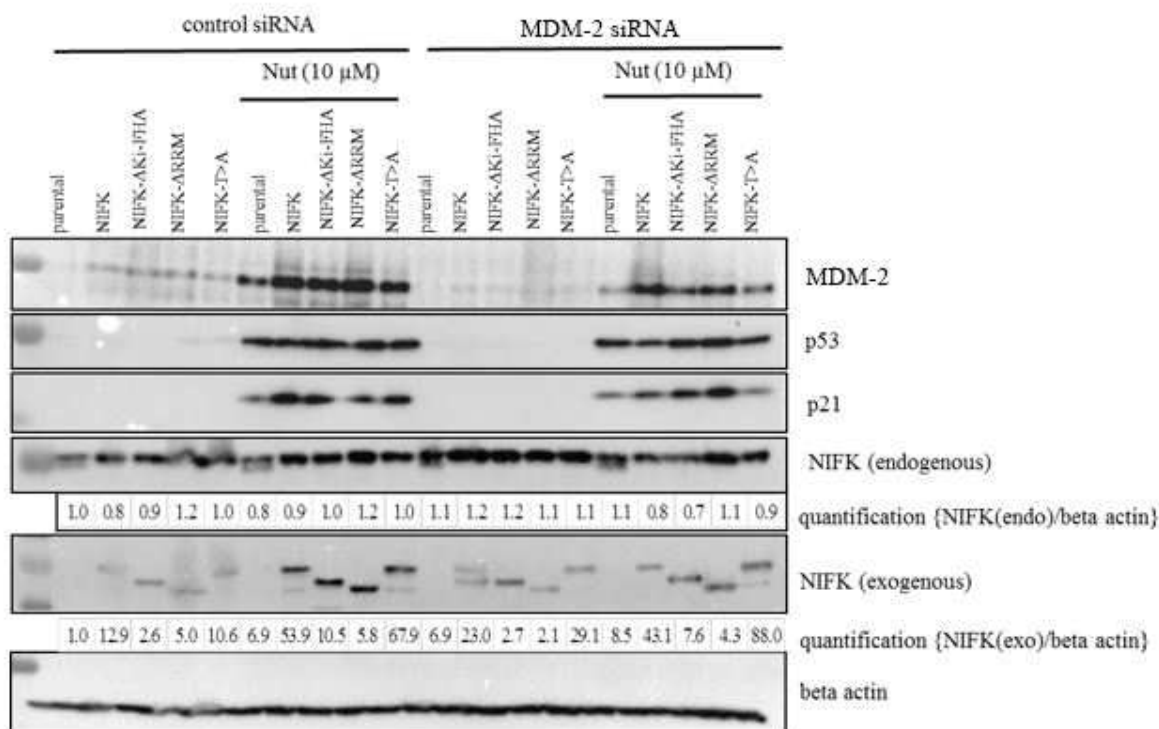
Figure 3.1.6 (F) Western Blot. *A2780 cells and the NIFK overexpression cells were infected with either control siRNA or MDM2 siRNA for 48 hours and were then subjected to either treatment with DMSO or Nutlin-3a (10µM) for 24 hours. The whole cell lysates were collected from the treated cells and were subjected to immunoblot using the different antibodies shown above. The ß-actin blot served as the loading control for all samples.*

si RNA	
Name	**Sequence**
hs.Ri.MDM2.13.1	5'-rGrCrArArCrUrUrUrArArUrGrGrUrA
hs.Ri.MDM2.13.1	5'-rGrCrArArCrUrUrUrArArUrGrGrUrA
hs.Ri.MDM2.13.2	5'-rGrUrArUrGrUrArGrArCrArArCrCrArArUrU
hs.Ri.MDM2.13.2	5'-rGrUrArUrGrUrArGrArCrArArCrCrArArUrU

Table 3.1.4. *Lists of Lists of MDM2 siRNA sequences used in transfection to A2780 and NIFK overexpression cells.*

3.1.7 Higher NIFK expression is associated with poor outcome in ovarian cancer patients.

We next determined the association between NIFK expression and clinical outcome in patients with ovarian cancer. Kaplan-Meier analyses of 1,657 ovarian tumor samples, provided by the online Kaplan-Meier (KM) plotter (Gyorffy et al. 2010), point out that in general higher expression of NIFK was associated with lower progression-free survival (PFS) and overall survival (OS) in ovarian cancer patients (Figure 3.1.7A and 3.1.7 B). The plots indicate that the ovarian cancers with higher NIFK expression are significantly associated with a poor response to the current chemotherapy, resulting in decreased progression-free and overall survival. These findings might be relevant towards improving our understand the pathogenesis of ovarian cancer given our forward genetic screening studies suggest a role of NIFK in a subset of ovarian cancer with wild-type p53.
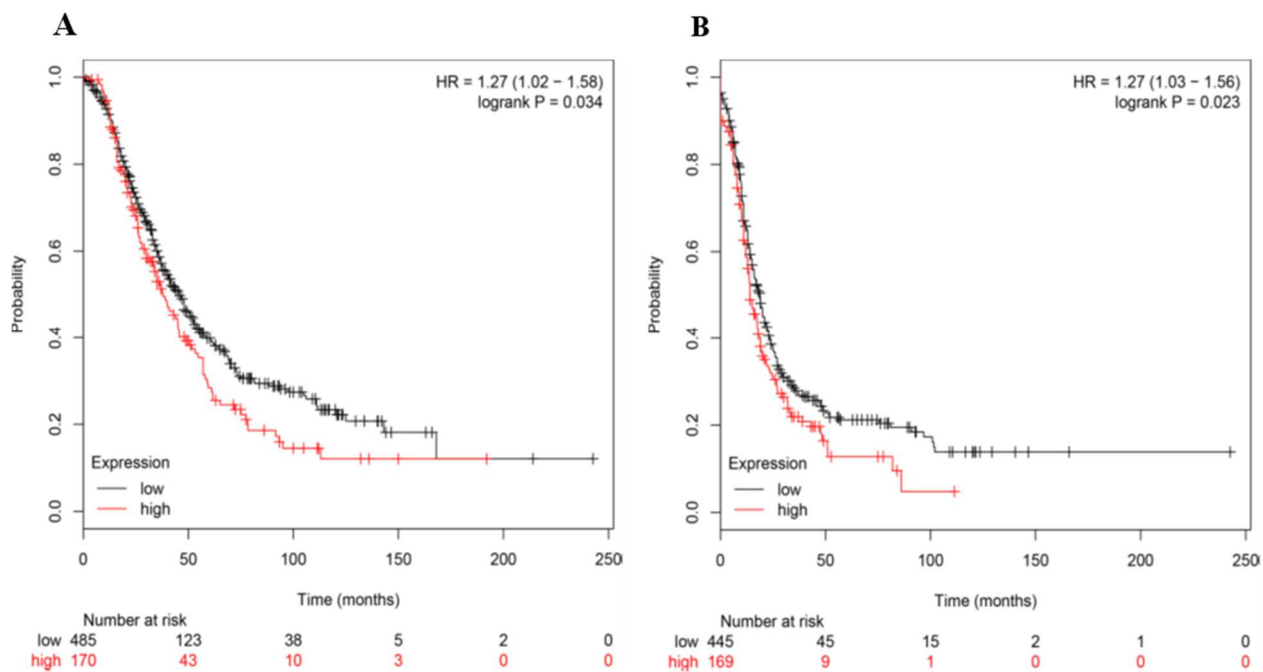
Figure 3.1.7 Association between NIFK expression and clinical outcome. *(A) Higher expression of NIFK in ovarian cancer is associated with poor overall survival. (B) Higher expression of NIFK in ovarian cancer is associated with early disease recurrence (progression-free survival).*

Chapter 4: Summary and Discussion

4.1 Summary

We derived an ovarian cancer cDNA library from patient samples and used it in a forward genetic screen in *TP53* wild-type ovarian cancer cells to identify the potential exogenous factors that negatively regulate p53 functions. First, we established an optimal transduction method to transduced retroviral particles into A2780 cells (Figure 3.1.2). Second, we established an optimal concentration of Nutlin-3a that can suppress clonogenic growth (Figure 3.1.3). Third, we established PCR conditions to rescue the transduced genes from the cDNA library (Figure 3.1.4). These experiments were essential to establish the necessary steps for a successful screening of the cDNA library. From these studies we identified NIFK as a potential negative regulator of p53 activity.

We also performed the colony formation assay using A2780 and NIFK overexpression A2780 cells (Figure 3.1.6). From the publish paper, FHA domain of NIFK is required to interact with Ki-67 protein and two phosphorylation sites Thr^{234} and Thr^{238} are needed for the interactions. Change of those two phosphorylation sites to alanine will terminate the interaction between Ki-67 and NIFK proteins and we used the construct NIFK-T>A to find out what is the important function of those in ovarian cancer. RNA reorganization motif (RRM) of NIFK is essential for the pre-rRNA processing and G1 progression (Pan et al. 2015). We included all four different constructs in our experiment to find out the role of NIFK in ovarian cancer. Our results showed that NIFK full length, NIFK-ΔKi-FHA, NIFK-ΔRRM, NIFK-T>A overexpressing cells are consistently more resistant to Nutlin-3a (Figure 3.1.6 A). We tested other genes that are transcriptionally regulated by p53, such as p21 and GADD45, by qRT-PCR and we found that there was no difference in these genes that are involved in cell cycle arrest

such as compare to A2780 and NIFK overexpression cells except GADD45. The GADD45 transcription was regulated by p53 after Nultin-3a treatment but the opposite result was observed in Western Blot (Figure 3.1.6 D & 3.1.6 E). Furthermore, we found that higher NIFK overexpression is associated with poor overall survival and disease-free survival in ovarian cancer patients (Figure 3.1.7). Our study identified for the first time a potential negative regulator of p53 and its network in cell cycle arrest and cell growth. However, additional studies are required to confirm that NIFK can negatively regulates p53 protein functions. Specifically, it will be important to identify the exact mechanism(s) of how NIFK regulates p53 functions and its network in ovarian cancer. We tried to use siRNA NIFK in the experiments to explore the role of NIFK in ovarian cancer. Unfortunately, NIFK knockdown with siRNA were unsuccessful due to very low efficiency in multiple set of siRNA. We also looked for ovarian cancer cell lines which have either low level expression or no expression of NIFK. All the ovarian cell lines we have showed the moderate to higher expression of NIFK by Western Blot (data not included). From our immunofluorescent data, NIFK-ΔRRM showed that the localization of NIFK protein to nucleoli was terminated and *NIFK-ΔRRM* protein was accumulated in the cytoplasm (data not included). From all of our experiment data pointed that NIFK is the novel gene that needs to investigate in detail to understand the mechanism in ovarian cancer. Nevertheless, our studies suggest that NIFK can play a role in the pathogenesis of ovarian cancer patients with functional wild-type p53.

4.2 Discussion

The FHA domains found in kinases, phosphatase, kinesins and transcription factor indicate the wide variety of functions of this domain. The FHA domain is particularly important in cell cycle control, DNA damage repair and cell proliferation. The nucleolar protein NIFK (MKI67IP) has a Ki-67 FHA binding domain as identified from a yeast two-hybrid screen. One study suggested that NIFK played a role in cell proliferation in Ki-67 dependent manner via CK1α and ß-catenin (Lin et al. 2016). The interaction between NIFK and Ki-67 FHA domain requires the phosphorylation on both Thr^{234} and Thr^{238} of NIFK (Takagi et al. 2001). The other domain of NIFK is RRM (RNA recognition motif) domain and previous studies have shown that the RRM domain is able to bind to double-stranded DNA sequences (Newberry, Latifi, and Towler 1999). Also from other studies, the RRM domain appears to be involved in the protein-protein interaction of post-transcriptional gene regulation as well as RNA recognition (Maris, Dominguez, and Allain 2005) (Kielkopf, Lucke, and Green 2004). All these studies along with our findings from the forward genetic screening indicate that NIFK is the candidate gene to study the cellular mechanism in ovarian cancer with functional p53 protein. The over-expressed NIFK cells were tested for its ability to promote growth under different concentrations of Nutlin-3a, and we found that NIFK-overexpressing cells formed colonies even in a higher concentration of Nutlin-3a (Figure 3.1.6). From our experiment, the protein level of GADD45 is slighter lower in NIFK overexpressed cells with Nutlin-3a treatment (Figure 3.1.6). In addition, the deletion of RRM (RNA recognition motif) domain results in localization of protein to cytoplasm instead of nucleoli (data not included). Our results raise the possibility that NIFK will play a role in tumor cell proliferation and may counteract the growth suppressive function of p53 protein. Additional

studies will be needed to further refine the function of NIFK in the development of certain forms of ovarian cancer.

References

Andersen, J. S., C. E. Lyon, A. H. Fox, A. K. Leung, Y. W. Lam, H. Steen, M. Mann, and A. I. Lamond. 2002. 'Directed proteomic analysis of the human nucleolus', *Curr Biol*, 12: 1-11.

Barak, Y., E. Gottlieb, T. Juven-Gershon, and M. Oren. 1994. 'Regulation of mdm2 expression by p53: alternative promoters produce transcripts with nonidentical translation potential', *Genes Dev*, 8: 1739-49.

Beckerman, R., and C. Prives. 2010. 'Transcriptional regulation by p53', *Cold Spring Harb Perspect Biol*, 2: a000935.

Bullwinkel, J., B. Baron-Luhr, A. Ludemann, C. Wohlenberg, J. Gerdes, and T. Scholzen. 2006. 'Ki-67 protein is associated with ribosomal RNA transcription in quiescent and proliferating cells', *J Cell Physiol*, 206: 624-35.

Buys, S. S., E. Partridge, A. Black, C. C. Johnson, L. Lamerato, C. Isaacs, D. J. Reding, R. T. Greenlee, L. A. Yokochi, B. Kessel, E. D. Crawford, T. R. Church, G. L. Andriole, J. L. Weissfeld, M. N. Fouad, D. Chia, B. O'Brien, L. R. Ragard, J. D. Clapp, J. M. Rathmell, T. L. Riley, P. Hartge, P. F. Pinsky, C. S. Zhu, G. Izmirlian, B. S. Kramer, A. B. Miller, J. L. Xu, P. C. Prorok, J. K. Gohagan, C. D. Berg, and Plco Project Team. 2011. 'Effect of screening on ovarian cancer mortality: the Prostate, Lung, Colorectal and Ovarian (PLCO) Cancer Screening Randomized Controlled Trial', *JAMA*, 305: 2295-303.

Chen, J., J. Lin, and A. J. Levine. 1995. 'Regulation of transcription functions of the p53 tumor suppressor by the mdm-2 oncogene', *Mol Med*, 1: 142-52.

Chen, J., V. Marechal, and A. J. Levine. 1993. 'Mapping of the p53 and mdm-2 interaction domains', *Mol Cell Biol*, 13: 4107-14.

Chen, L., V. Marechal, J. Moreau, A. J. Levine, and J. Chen. 1997. 'Proteolytic cleavage of the mdm2 oncoprotein during apoptosis', *J Biol Chem*, 272: 22966-73.

Domcke, S., R. Sinha, D. A. Levine, C. Sander, and N. Schultz. 2013. 'Evaluating cell lines as tumour models by comparison of genomic profiles', *Nat Commun*, 4: 2126.

el-Deiry, W. S., S. E. Kern, J. A. Pietenpol, K. W. Kinzler, and B. Vogelstein. 1992. 'Definition of a consensus binding site for p53', *Nat Genet*, 1: 45-9.

Erickson, B. K., M. G. Conner, and C. N. Landen, Jr. 2013. 'The role of the fallopian tube in the origin of ovarian cancer', *Am J Obstet Gynecol*, 209: 409-14.

George, S. H., R. Garcia, and B. M. Slomovitz. 2016. 'Ovarian Cancer: The Fallopian Tube as the Site of Origin and Opportunities for Prevention', *Front Oncol*, 6: 108.

Gerdes, J., H. Lemke, H. Baisch, H. H. Wacker, U. Schwab, and H. Stein. 1984. 'Cell cycle analysis of a cell proliferation-associated human nuclear antigen defined by the monoclonal antibody Ki-67', *J Immunol*, 133: 1710-5.

Gyorffy, B., A. Lanczky, A. C. Eklund, C. Denkert, J. Budczies, Q. Li, and Z. Szallasi. 2010. 'An online survival analysis tool to rapidly assess the effect of 22,277 genes on breast cancer prognosis using microarray data of 1,809 patients', *Breast Cancer Res Treat*, 123: 725-31.

Haupt, Y., R. Maya, A. Kazaz, and M. Oren. 1997. 'Mdm2 promotes the rapid degradation of p53', *Nature*, 387: 296-9.

Honda, R., H. Tanaka, and H. Yasuda. 1997. 'Oncoprotein MDM2 is a ubiquitin ligase E3 for tumor suppressor p53', *FEBS Lett*, 420: 25-7.

Jones, S. N., A. E. Roe, L. A. Donehower, and A. Bradley. 1995. 'Rescue of embryonic lethality in Mdm2-deficient mice by absence of p53', *Nature*, 378: 206-8.

Jones, S., T. L. Wang, R. J. Kurman, K. Nakayama, V. E. Velculescu, B. Vogelstein, K. W. Kinzler, N. Papadopoulos, and M. Shih Ie. 2012. 'Low-grade serous carcinomas of the ovary contain very few point mutations', *J Pathol*, 226: 413-20.

Kielkopf, C. L., S. Lucke, and M. R. Green. 2004. 'U2AF homology motifs: protein recognition in the RRM world', *Genes Dev*, 18: 1513-26.

Kruse, J. P., and W. Gu. 2009. 'Modes of p53 regulation', *Cell*, 137: 609-22.

Kubbutat, M. H., S. N. Jones, and K. H. Vousden. 1997. 'Regulation of p53 stability by Mdm2', *Nature*, 387: 299-303.

Kurman, R. J., and M. Shih Ie. 2010. 'The origin and pathogenesis of epithelial ovarian cancer: a proposed unifying theory', *Am J Surg Pathol*, 34: 433-43.

———. 2011. 'Molecular pathogenesis and extraovarian origin of epithelial ovarian cancer--shifting the paradigm', *Hum Pathol*, 42: 918-31.

———. 2016. 'The Dualistic Model of Ovarian Carcinogenesis: Revisited, Revised, and Expanded', *Am J Pathol*, 186: 733-47.

Kussie, P. H., S. Gorina, V. Marechal, B. Elenbaas, J. Moreau, A. J. Levine, and N. P. Pavletich. 1996. 'Structure of the MDM2 oncoprotein bound to the p53 tumor suppressor transactivation domain', *Science*, 274: 948-53.

Levine, A. J. 1997. 'p53, the cellular gatekeeper for growth and division', *Cell*, 88: 323-31.

Levine, A. J., J. Momand, and C. A. Finlay. 1991. 'The p53 tumour suppressor gene', *Nature*, 351: 453-6.

Li, H., I. J. Byeon, Y. Ju, and M. D. Tsai. 2004. 'Structure of human Ki67 FHA domain and its binding to a phosphoprotein fragment from hNIFK reveal unique recognition sites and new views to the structural basis of FHA domain functions', *J Mol Biol*, 335: 371-81.

Lin, T. C., C. Y. Su, P. Y. Wu, T. C. Lai, W. A. Pan, Y. H. Jan, Y. C. Chang, C. T. Yeh, C. L. Chen, L. P. Ger, H. T. Chang, C. J. Yang, M. S. Huang, Y. P. Liu, Y. F. Lin, J. Y. Shyy, M. D. Tsai, and M. Hsiao. 2016. 'The nucleolar protein NIFK promotes cancer progression via CK1alpha/beta-catenin in metastasis and Ki-67-dependent cell proliferation', *Elife*, 5.

Marechal, V., B. Elenbaas, L. Taneyhill, J. Piette, M. Mechali, J. C. Nicolas, A. J. Levine, and J. Moreau. 1997. 'Conservation of structural domains and biochemical activities of the MDM2 protein from Xenopus laevis', *Oncogene*, 14: 1427-33.

Maris, C., C. Dominguez, and F. H. Allain. 2005. 'The RNA recognition motif, a plastic RNA-binding platform to regulate post-transcriptional gene expression', *Febs j*, 272: 2118-31.

May, P., and E. May. 1999. 'Twenty years of p53 research: structural and functional aspects of the p53 protein', *Oncogene*, 18: 7621-36.

Mirza, M. R., B. J. Monk, J. Herrstedt, A. M. Oza, S. Mahner, A. Redondo, M. Fabbro, J. A. Ledermann, D. Lorusso, I. Vergote, N. E. Ben-Baruch, C. Marth, R. Madry, R. D. Christensen, J. S. Berek, A. Dorum, A. V. Tinker, A. du Bois, A. Gonzalez-Martin, P. Follana, B. Benigno, P. Rosenberg, L. Gilbert, B. J. Rimel, J. Buscema, J. P. Balser, S. Agarwal, and U. A. Matulonis. 2016. 'Niraparib Maintenance Therapy in Platinum-Sensitive, Recurrent Ovarian Cancer', *N Engl J Med*, 375: 2154-64.

Mittica, G., E. Ghisoni, G. Giannone, S. Genta, M. Aglietta, A. Sapino, and G. Valabrega. 2018. 'PARP Inhibitors in Ovarian Cancer', *Recent Pat Anticancer Drug Discov*, 13: 392-410.

Montes de Oca Luna, R., D. S. Wagner, and G. Lozano. 1995. 'Rescue of early embryonic lethality in mdm2-deficient mice by deletion of p53', *Nature*, 378: 203-6.

Newberry, E. P., T. Latifi, and D. A. Towler. 1999. 'The RRM domain of MINT, a novel Msx2 binding protein, recognizes and regulates the rat osteocalcin promoter', *Biochemistry*, 38: 10678-90.

Oda, K., H. Arakawa, T. Tanaka, K. Matsuda, C. Tanikawa, T. Mori, H. Nishimori, K. Tamai, T. Tokino, Y. Nakamura, and Y. Taya. 2000. 'p53AIP1, a potential mediator of p53-dependent apoptosis, and its regulation by Ser-46-phosphorylated p53', *Cell*, 102: 849-62.

Okoshi, R., T. Ozaki, H. Yamamoto, K. Ando, N. Koida, S. Ono, T. Koda, T. Kamijo, A. Nakagawara, and H. Kizaki. 2008. 'Activation of AMP-activated protein kinase induces p53-dependent apoptotic cell death in response to energetic stress', *J Biol Chem*, 283: 3979-87.

Oren, M. 1999. 'Regulation of the p53 tumor suppressor protein', *J Biol Chem*, 274: 36031-4.

Pan, W. A., H. Y. Tsai, S. C. Wang, M. Hsiao, P. Y. Wu, and M. D. Tsai. 2015. 'The RNA recognition motif of NIFK is required for rRNA maturation during cell cycle progression', *RNA Biol*, 12: 255-67.

Parada, L. F., C. J. Tabin, C. Shih, and R. A. Weinberg. 1982. 'Human EJ bladder carcinoma oncogene is homologue of Harvey sarcoma virus ras gene', *Nature*, 297: 474-8.

Prat, J. 2015. 'FIGO's staging classification for cancer of the ovary, fallopian tube, and peritoneum: abridged republication', *J Gynecol Oncol*, 26: 87-9.

Roth, J., M. Dobbelstein, D. A. Freedman, T. Shenk, and A. J. Levine. 1998. 'Nucleo-cytoplasmic shuttling of the hdm2 oncoprotein regulates the levels of the p53 protein via a pathway used by the human immunodeficiency virus rev protein', *Embo j*, 17: 554-64.

Ruppert, J. M., and B. Stillman. 1993. 'Analysis of a protein-binding domain of p53', *Mol Cell Biol*, 13: 3811-20.

Siegel, R. L., K. D. Miller, and A. Jemal. 2018. 'Cancer statistics, 2018', *CA Cancer J Clin*, 68: 7-30.

Skates, S. J., M. H. Greene, S. S. Buys, P. L. Mai, P. Brown, M. Piedmonte, G. Rodriguez, J. O. Schorge, M. Sherman, M. B. Daly, T. Rutherford, W. R. Brewster, D. M. O'Malley, E. Partridge, J. Boggess, C. W. Drescher, C. Isaacs, A. Berchuck, S. Domchek, S. A. Davidson, R. Edwards, S. A. Elg, K. Wakeley, K. A. Phillips, D. Armstrong, I. Horowitz, C. J. Fabian, J. Walker, P. M. Sluss, W. Welch, L. Minasian, N. K. Horick, C. H. Kasten, S. Nayfield, D. Alberts, D. M. Finkelstein, and K. H. Lu. 2017. 'Early Detection of Ovarian Cancer using the Risk of Ovarian Cancer Algorithm with Frequent CA125 Testing in Women at Increased Familial Risk - Combined Results from Two Screening Trials', *Clin Cancer Res*, 23: 3628-37.

Taira, N., K. Nihira, T. Yamaguchi, Y. Miki, and K. Yoshida. 2007. 'DYRK2 is targeted to the nucleus and controls p53 via Ser46 phosphorylation in the apoptotic response to DNA damage', *Mol Cell*, 25: 725-38.

Takagi, M., M. Sueishi, T. Saiwaki, A. Kametaka, and Y. Yoneda. 2001. 'A novel nucleolar protein, NIFK, interacts with the forkhead associated domain of Ki-67 antigen in mitosis', *J Biol Chem*, 276: 25386-91.

Thut, C. J., J. L. Chen, R. Klemm, and R. Tjian. 1995. 'p53 transcriptional activation mediated by coactivators TAFII40 and TAFII60', *Science*, 267: 100-4.

Vassilev, L. T., B. T. Vu, B. Graves, D. Carvajal, F. Podlaski, Z. Filipovic, N. Kong, U. Kammlott, C. Lukacs, C. Klein, N. Fotouhi, and E. A. Liu. 2004. 'In vivo activation of the p53 pathway by small-molecule antagonists of MDM2', *Science*, 303: 844-8.

Verheijen, R., H. J. Kuijpers, R. O. Schlingemann, A. L. Boehmer, R. van Driel, G. J. Brakenhoff, and F. C. Ramaekers. 1989. 'Ki-67 detects a nuclear matrix-associated proliferation-related antigen. I. Intracellular localization during interphase', *J Cell Sci*, 92 (Pt 1): 123-30.

Vogelstein, B., D. Lane, and A. J. Levine. 2000. 'Surfing the p53 network', *Nature*, 408: 307-10.

Vousden, K. H., and X. Lu. 2002. 'Live or let die: the cell's response to p53', *Nat Rev Cancer*, 2: 594-604.